https://doi.org/10.5194/essd-2021-470
Preprint. Discussion started: 16 May 2022

Open Access Earth System Science Data Discussions

High-resolution water level and storage variation datasets for 338 reservoirs in China during 2010–2020

Youjiang Shen[1], Dedi Liu[1], Liguang Jiang[2], Karina Nielsen[3], Jiabo Yin[1], Jun Liu[4], Peter Bauer-Gottwein[4]

[1]State Key Laboratory of Water Resources & Hydropower Engineering Science, Wuhan University, Wuhan, 430072, China
[2]School of Environmental Science and Engineering, Southern University of Science and Technology, Shenzhen, 518055, China
[3]DTU Space, National Space Institute, Technical University of Denmark, 2800, Kongens Lyngby, Denmark
[4]Department of Environmental Engineering, Technical University of Denmark, 2800, Kongens Lyngby, Denmark

Correspondence to: Dedi Liu (dediliu@whu.edu.cn)

Abstract. Reservoirs and dams are essential infrastructures in water management, thus information of their surface water area (SWA), water surface elevation (WSE), and reservoir water storage change (RWSC), is crucial for understanding their properties and interactions on hydrological and biogeochemical cycles. However, knowledge of these reservoir characteristics is scarce or inconsistent at national scale. Here, we introduce comprehensive reservoir datasets of 338 reservoirs in China, with a total of 470.6 km^3 storage capacity (50% Chinese reservoir storage capacity). Given the scarcity of publicly available gauged observations and operational applications of satellites for hydrological cycles, we utilize multiple satellite altimetry missions (SARAL/AltiKa, Sentinel-3 A and B, and CroySat-2) and Landsat satellite data to produce a comprehensive reservoir dataset on the WSE, SWA, and RWSC during 2010–2020. Validation against gauged measurements of 93 reservoirs demonstrates the relatively high accuracy and reliability of our remotely-sensed datasets: (1) Across gauge comparisons of RWSC, the median statistics of CC, NRMSE, and RMSE are 0.76, 15%, and 0.035 km^3, with a total of 75% validated reservoirs (70 of 93) having good RMSE from 0.002 to 0.35 km^3 and NRMSE values smaller than 20%. (2) Comparisons of WSE retracked by four satellite altimeters and gauges show good agreement. Specifically, percentages of reservoirs having good and moderate RMSE values smaller than 1.0 m for CryoSat-2 (validated in 30 reservoirs), SARAL/AltiKa (8), Sentinel-3A (25), and Sentinel-3B (25) are 90%, 88%, 64%, and 76% respectively. By taking advantages of four satellite altimetry missions, we are able to densify WSE observations across spatiotemporal scales. Statistically, around 85% validated reservoirs (53 of 62) have RMSE values below 1.0 m, while 63% reservoirs (39 of 62) have a good data quality with RMSE values below 0.6 m. Overall, our study fills such a data gap with regard to comprehensive reservoir information in China and provides strong support for many aspects such as hydrological processes, water resources, and other studies. The dataset is publicly available on Zenodo at https://doi.org/10.5281/zenodo.5812012 (Shen et al., 2021).

https://doi.org/10.5194/essd-2021-470
Preprint. Discussion started: 16 May 2022

Open Access Earth System Science Data Discussions

1 Introduction

Reservoirs and dams are essential infrastructures in water management that alters the natural river flows to provide services such as flood control, hydroelectricity generation and irrigation (Intralawan et al., 2018; Zhu et al., 2020). Largely mandated by the Flood Control Act of 1950, more than 98,000 reservoirs and dams have been constructed in China with a total water capacity of around 932 km^3 (Statistic Bulletin on China Water Activities, 2018). The boom of dam impoundment will continue for next decades in the background of climate warming and human activities (Lehner et al., 2011; Gutenson et al., 2020). Understanding the role of reservoirs and dams in the hydrological cycles has become increasingly important (Buccola et al., 2016; Marx et al., 2017; Chaudhari et al., 2018; Busker et al., 2019). Our review of the literature suggests that a combination of data and river models is the core to understand impacts of reservoirs on hydrological cycles. However, most studies on reservoirs have been significantly limited to data scarcity. Despite progress in process-based models with new reservoir schemes and hyper spatial resolution (Shin et al., 2019; Dang et al., 2020), most of them had approximated the reservoir releases just through storage-release equations and routed downstream with river routing mechanisms (e.g., Zhao et al., 2016; Zajac et al., 2017; Pokhrel et al., 2018; Yassin et al., 2019; Boulange et al., 2021). Acknowledging such approximations, we intend to contribute relevant studies by introducing the remotely-sensed reservoir datasets that can be applied as constraints to calibrate models or directly used for reservoir analysis. Our study plans to fill such a data gap, i.e., to develop the remotely-sensed reservoir datasets including surface water area (SWA), water surface elevation (WSE), and reservoir water storage change (RWSC) of 338 reservoirs in China.

Due to the absence of observational records describing the multitude of reservoir characteristics, remote sensing techniques have been developed to monitor reservoirs and have characterized reservoir across the globe (Gao et al., 2012; Duan and Bastiaanssen, 2013). Satellite missions have been used to offer reliable reservoir estimates such as SWA, WSE, and RWSC (Zhang et al., 2014; Wang et al., 2020; Zhang et al., 2020, Shen et al., 2022). WSE can be acquired by satellite laser or radar altimetry missions such as Sentinel-3A/B, CryoSat-2, Jason-1/2/3, and ICESat-1/2 (e.g., Wingham et al., 2006; Donlon et al., 2011; Zhang et al., 2011; Song et al., 2013; Jiang et al., 2020); SWA can be derived from SAR or optical images from e.g. MODIS, Landsat MSS/TM/OLI and Sentinel-1/2 (e.g., Goumehei et al., 2019; Weekley and Li, 2019); and RWSC can be calculated by two methods: one is using the overlapped measurements of SWA and WSE from different satellite missions, and the other one is constructing hypsometry relationships, i.e., Area-Elevation curves (A–E) derived from satellite measurements (Bonnema et al., 2016). There have been studies and online databases producing the remotely-sensed datasets for inland reservoirs/lakes at regional/global scales (Birkett et al., 2011; Crétaux et al., 2011; Gao et al., 2012; Zhang et al., 2014; Khandelwal et al., 2017; Getirana et al., 2018; Busker et al., 2019; Yao et al., 2019; Zhao and Gao, 2019; Li et al., 2020; Tortini et al., 2020). We have listed the studies and databases in Table 1 to summarize the progress of remotely-sensed data of reservoirs. It is obvious that there is a data gap on national information of consistent reservoir datasets. Records of a few reservoirs are available from these databases or previous studies. For example, approximately 30 Chinese reservoirs are

https://doi.org/10.5194/essd-2021-470
Preprint. Discussion started: 16 May 2022

available from three datasets (Hydroweb, G-REALM and DAHITI). Therefore, studies dynamically incorporating various satellites into a comprehensive reservoir data set at national scale can fill the data gap.

With this motivation in mind, we further identified some limitations of the studies listed in Table 1. Most of them just focus on developing a single reservoir data set (WSE, SWA, RWSC, or A–E relationships) for a few reservoirs across the globe (Gao et al., 2012; Mu et al., 2020; Zhang et al., 2014). For example, Yao et al. (2019) constructs the long-term area time series for 428 reservoirs and lakes at bi-monthly scale by recovering inundation areas from contaminated Landsat-based images. The remotely-sensed products had often not been validated by ground observed data owing to the lack of large observations, with the exception of a few studies with scare in-situ observations (Bonnema and Hossain, 2019). Khandelwal et al. (2017) mapped the global areal extent and temporal variations of reservoirs at 500 m spatial resolution, eight-day intervals from 2000 to 2015. However, their datasets are simply validated on 94 reservoirs by comparing SWA with altimetry measurements, whose accuracy remains questionable. Tortini et al. (2020) provides a global data set of SWA, WSE, and storage change over 347 lakes/reservoirs, but results are validated at only one lake. Moreover, the remotely-sensed datasets (e.g., lake/reservoir storage variations by Busker et al., 2019 or RWSC by Avisse et al., 2017) are difficult to be accessed. A geo-statistical approach has also been adopted to estimate RWSC with a surface water area during 1985–2005 (Fang et al., 2019), there are critical limitations shown as wide confidence intervals and high uncertainties due to its simplifications. There are several databases offering the time series of altimetry-derived WSE and/or imagery-based SWA estimates for big reservoirs across the globe. They are the Hydroweb (Crétaux et al., 2011), the G-REALM (Birkett et al., 2011), the Hydrosat, the DAHITI (Schwatke et al., 2015), the Bluedot observatory and others. These databases incorporated more altimetric information and provided datasets at higher temporal resolution. For example, Hydroweb firstly provided altimetry-derived water level time series on lakes and rivers from different satellite missions. Unlike Hydroweb, G-REALM focuses on some of the world's largest reservoirs/lakes. Within a rather unprecedented framework of online web application, Bluedot observatory allows for exploring and generating imagery-based SWA time series of reservoirs/lakes on-the-fly. As already mentioned, records of a few reservoirs in China are available. Whether reservoir water level time series from these three databases have a good agreement with one another and gauged measurements is not systematically evaluated, which can be shown in this study.

In light of the above, our objective is to fill research gap with regard to comprehensive reservoir information in China, thus supporting process-based models to better understand systematic reservoir effects. To densify reservoir observations, multiple satellite altimetry missions (Sentinel-3 A/B, SARAL/AltiKa, and CroySat-2) and Landsat data are utilized to develop high-resolution remotely-sensed reservoir datasets including SWA, WSE, and RWSC of 338 reservoirs in China during 2010–2020, with a total of 470.6 km^3 water capacity (50% reservoir water capacity in China). To validate the remotely-sensed results, the in-situ observations of 93 reservoirs are used for evaluations, thereby bringing the highest level of confidence on the quality and novelty of datasets. Users are free to access datasets in an easily readable file format that allows researchers quickly handle our datasets at https://doi.org/10.5281/zenodo.5812012 (Shen et al., 2021).

Results of this study align with the efforts to understand role of reservoirs on hydrological cycles but significantly limited to data scarcity. Moreover, a growing interest in using remote-sensing data in hydrological cycle is expected, thus knowing the

https://doi.org/10.5194/essd-2021-470
Preprint. Discussion started: 16 May 2022


Open Access Earth System Science Data Discussions

accuracy of the remote-sensing data is a prerequisite. Although previous studies assessed satellite altimeters in retrieving reservoir water levels (Shu et al., 2021), knowledge is still limited as to evaluations of different altimeters for a large sample of reservoirs, which can be shown in this study. Overall, our unique contribution lies in the unique and novel remotely-sensed datasets to fill a data gap with regard to comprehensive reservoir information in China, and to benefit studies involving many fields such as hydrological processes, water resources, and other studies.

https://doi.org/10.5194/essd-2021-470
Preprint. Discussion started: 16 May 2022

Open Access Earth System Science Data Discussions

Table 1. Summary of recent studies and databases producing the remotely-sensed data on surface water area (A), water surface elevation (H), storage variation (V), and hypsometric curve of reservoirs.

Reference	No. of reservoirs (China)	Data type	Time and temporal resolution	Source data and description
Gao et al. (2012)	34 (0)	H, A, V, and hypsometric curve (not publicly accessible)	1992–2010 Sub-monthly/monthly	Altimetry data: online databases from a combination of five satellite altimeters Optical data: MODIS (Moderate Resolution Imaging Spectroradiometer) Validated in 5 reservoirs
Zhang et al. (2014)	21 (0)	A, V, and hypsometric curve	2000–2012 Sub-monthly/monthly	Altimetry data: ICESat/Geoscience Laser Altimeter System Optical data: MODIS Validated in 5 reservoirs
Khandelwal et al. (2017)	94 (0)	A	2000–2015 Sub-monthly	Altimetry data: three online databases Optical data: MODIS Validated area time series against altimetry data
Yigzaw et al. (2018)	6800 (~900)	hypsometric curve	/	GRanD database Derived from an optimal geometric shape
Busker et al. (2019)	137 lakes and reservoirs (<4)	A, V, and hypsometric curve (not publicly accessible)	1984–2015 monthly	Altimetry data: DAHITI database Optical data: JRC Global Surface Water Data Validate area time series against altimetry data
Yao et al. (2019)	205 (~8)	A	1992–2018 Sub-monthly/monthly	Altimetry data: three online databases Optical data: Landsat Validated volume in 18 lakes
Liu et al. (2020)	24 (24)	A and V (not publicly accessible)	2004–2020 monthly	Altimetry data: Sentinel-3 Optical data: GRAS-approach area data
Tortini et al. (2020)	347 lakes and reservoirs (<10)	H, A, V, and hypsometric curve	1992–2018 Sub-monthly/monthly	Altimetry data: TOPEX/Poseidon, Jason-1/-2/-3, and Envisat Optical data: MODIS Validated in 1 lake
G-REALM	(~30)	H	1992–2021, 10–35 day	https://ipad.fas.usda.gov/cropexplorer/global_reservoir/
DAHITI	(8)	H	2002–2021, 10–35 day	https://dahiti.dgfi.tum.de/en/
Hydroweb	(32)	H, A	1992–2021, 10–35 day	http://hydroweb.theia-land.fr/
Bluedot	/	A	2016–2021, Sub-monthly	https://blue-dot-observatory.com/
Our study	(338)	H, A, V, and hypsometric curve	2010–2020 monthly	Altimetry data: CroySat-2, Sentinel-3A, Sentinel-3B, and SARAL/AltiKa Optical data: JRC Global Surface Water Data Validated in 93 reservoirs

2 Data and Methods

China has an enormous network of reservoirs across different geographical landscapes. In this study, we selected all reservoirs for which geographical information is available from the GRanD database (http://globaldamwatch.org/grand/, Lehner et al., 2011). The GRanD provides an extensive number of attributes for reservoir shapefiles including: geolocations of dams (i.e., latitude and longitude), extents and areas of reservoirs, dam heights, storage capacity and others. We found that there is a considerable variation in regulation capacity, water area, storage capacity, main function, and installed capacity to generate hydropower. Fig. 1 shows the spatial distribution of the final retained reservoirs and the coverage of both altimetry passes and

https://doi.org/10.5194/essd-2021-470
Preprint. Discussion started: 16 May 2022

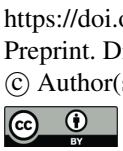

in-situ gauges as a reference for validation. Most reservoirs are densely grouped over eastern and middle China. These in-situ gauges provide a good bed to evaluate performance of each altimetry over diverse reservoirs. Furthermore, to densify altimetric observations, merging data from these missions is meaningful given that altimetry tracks are sparse. Poorly gauged or inaccessible reservoirs are the regions where satellite altimeters show the highest value.

We obtained daily water level and storage data spanning 2015–May 2021 for 93 reservoirs from the local watershed agency (http://xxfb.mwr.cn/index.html) and National Hydrological Information Centre for validation (http://113.57.190.228:8001/web/Report/BigMSKReport). All records follow a strict quality control, and the time series cover different periods. Data from May 2018 to June 2019 are missing for nearly all 93 reservoirs. 49 reservoirs cover the period of 2015–May 2021, while the remaining reservoirs cover the period of July 2019–May 2021. Each reservoir has a storage capacity more than 40 million m^3, with a total water capacity of 189.2 km^3.

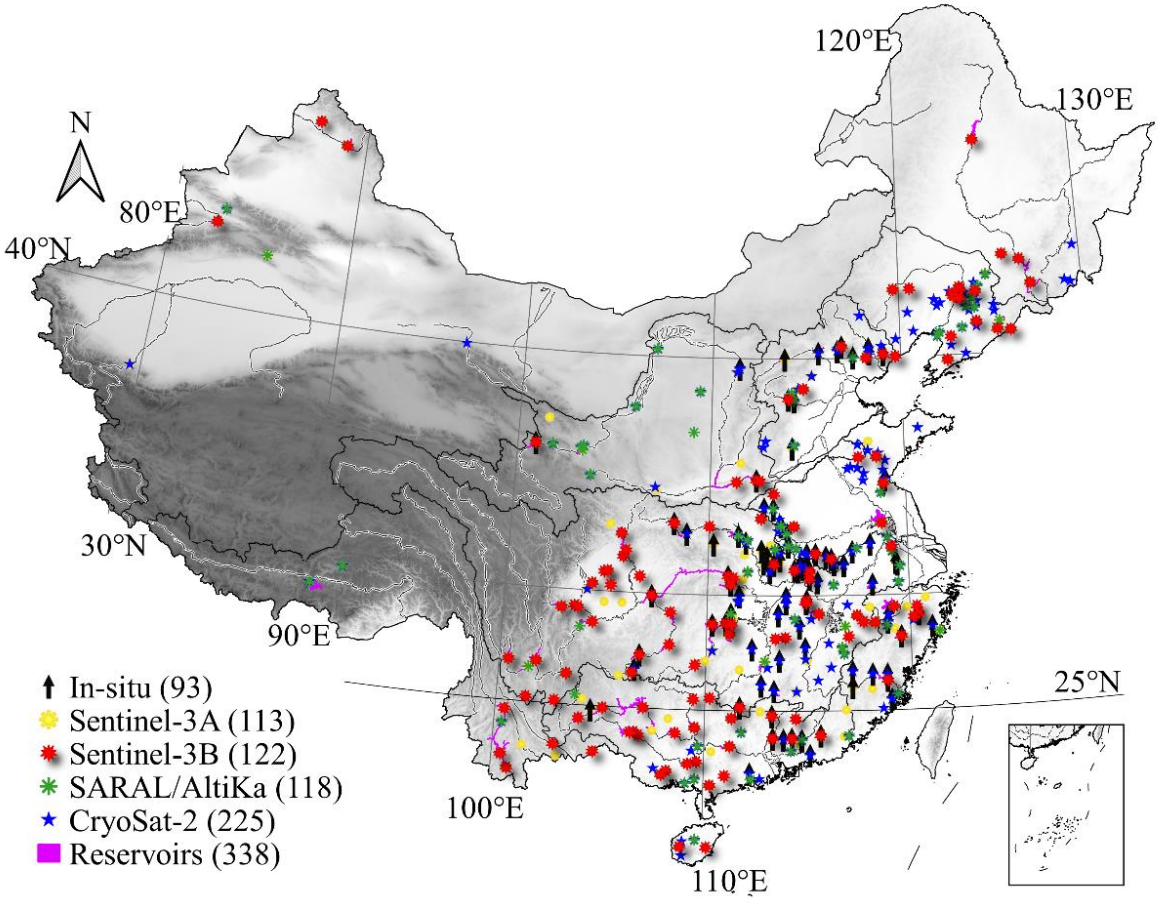

Figure 1: Map of reservoirs covered by multisource satellite altimeters and stages. 338 reservoirs are finally retained in our datasets. For more details, please refer to Sect. 3.1.

https://doi.org/10.5194/essd-2021-470
Preprint. Discussion started: 16 May 2022

2.1 Satellite radar altimetry

We collect satellite altimetry-derived WSE measurements from CroySat-2, Sentinel-3 A/B, and SARAL/AltiKa. For readers to get a broad understanding of these missions, the main features are summarized below while detailed information is available at the Official User Books (European Space Agency and Mullar Space Science Laboratory, 2012; Dinardo et al., 2018). CryoSat-2 (CS2) launched in April 2010 carries a Synthetic Aperture Interferometric Radar Altimeter. It operates in three modes, i.e., low resolution mode, synthetic aperture mode, and synthetic aperture interferometric mode. The baseline C level 1b dataset are from ESA (https://science-pds.cryosat.esa.int/), which provides 20 Hz measurements including waveforms, position, corrections, interferometric phase difference, etc. These waveforms were retracked with the Primary Peak Center Of Gravity (PPCOG), Narrow Primary Peak Threshold Retracker with a 50% (NPPTr[0.5]) and 80% (NPPTr[0.8]) threshold algorithms (Jain et al., 2015). SARAL/AltiKa is the first altimeter operating in Ka-band frequency, which results in higher spatial resolution and leads to higher data availability (CNES, 2016). Geophysical Data Records (GDRs) of SARAL/AltiKa are downloaded from CNES AVISO+ (ftp://avisoftp.cnes.fr/AVISO/pub/). The records provide ranges retracked using the Ice-1 and Ice-2 algorithms, and we also implemented the PPCOG, NPPTr[0.5] and NPPTr[0.8] algorithms to derive WSE. Sentinel-3 consists of the constellations of two satellites, i.e., Sentinel-3A (S3A) and Sentinel-3B (S3B), which were launched on February 2016 and April 2018, respectively. It is the first altimeter measuring in SAR radar altimeter at global scale with an open-loop tracking system. Therefore, it facilitates water measurement by increasing along-track resolution, accuracy and data availability. We downloaded Level 2 “Enhanced measurements” datasets from https://scihub.copernicus.eu/dhus/. It contains 20 Hz measurements with waveforms, altitude, position, corrections, and ranges retracked by the Ocean algorithm. We also implemented the PPCOG, NPPTr[0.5] and NPPTr[0.8] algorithms, and the traditional Offset Center Of Gravity (OCOG) algorithms to derive water level. All altimetry data are then referenced to the EGM2008 (Pavlis et al., 2012) geoid model. The source and version of each altimetry product are listed in Table 2.

Table 2. Summary of altimetry datasets used in this study.

Satellite	Data period	Retrackers	Repeat cycle
CryoSat-2	2010-2020.12	PPCOG, NPPTr[0.5], NPPTr[0.8]	369 day
SARAL/AltiKa	2016-2020.12	ICE-1, ICE-2, PPCOG, NPPTr[0.5], NPPTr[0.8]	-
Sentinel-3A	2016.2-2020.12	OCOG, Ocean, PPCOG, NPPTr[0.5], NPPTr[0.8]	27 day
Sentinel-3B	2018.4-2020.12	OCOG, Ocean, PPCOG, NPPTr[0.5], NPPTr[0.8]	27 day

Note: PPCOG refers to the Primary Peak Center Of Gravity algorithm. NPPTr[0.5] and NPPTr[0.8] refers to the Narrow Primary Peak Threshold retracker with a 50% and 80% threshold level algorithm, respectively. OCOG refers to the traditional Offset Center Of Gravity algorithm.

The first step of deriving satellite altimetry water levels is to select correct ground tracks and valid footprints falling on reservoirs. Altimetry data over the GRanD polygons of reservoirs intersected by ground tracks are extracted. After picking out valid footprints, WSE are constructed via the following equations:

https://doi.org/10.5194/essd-2021-470
Preprint. Discussion started: 16 May 2022


Open Access Earth System Science Data Discussions

$$WSE = H_{alt} - R_{range} - N_{geo}, \quad (1)$$

$$R_{range} = R_{trac} + R_{retrac} + R_{atm} + R_{geo}, \quad (2)$$

where H_{alt} refers to the altitude of satellite, N_{geo} is the height of EGM2008 geoid, and R_{range} is the range that measures the distance from water to satellite. R_{trac} is the range to the nominal bin of the waveform and R_{retrac} denotes the re-tracking correction. R_{atm} and R_{geo} are the atmospheric corrections (wet tropospheric, dry tropospheric, and ionospheric corrections) and the geophysical corrections (solid earth, pole, and ocean loading tides).

To analyze reservoir WSE variations, altimetry data have to be further processed to construct time series. Detailed procedures are as follows. Firstly, the altimetry-derived WSE are pre-selected based on the water occurrence map (occurrence > 10%) of the Global Surface Water Explorer (https://global-surface-water.appspot.com/). Secondly, we removed outliers for each pass (i.e., 2 deviations away from the median value) using the median of absolute deviation (Jiang et al., 2019). Thirdly, outliers are identified and discarded by comparing with SRTM DEM, i.e., 20 m away from DEM (40 m for reservoirs with large fluctuations). Fourthly, the remaining WSE measurements are applied to construct time series based on the R package "tsHydro" available from (https://github.com/cavios/tshydro). This package efficiently estimates along-track water level in the case of outlying measurements (Nielsen et al., 2015). After deriving WSE time series for each altimetry, we merge all time-series for a specific reservoir from multisource (CryoSat-2, S3A, S3B, and SARAL/AltiKa) if available. To remove systematic biases, Sentinel-3 data are set as the first baseline to remove the difference of the mean values of the two products during the overlap periods, because Sentinel-3 data are at higher temporal resolution than others. In cases where no data are available from Sentinel-3, CryoSat-2 data are set as the baseline. Then, the merged products are used for further RWSC estimates.

2.2 Surface area datasets

For SWA dynamics of reservoirs, we used the Joint Research Centre Global Surface Water Dataset version 1.3 (JRC-GSWD) available at https://global-surface-water.appspot.com/. Each pixel was individually classified into water, non-water, and no data, and the results are subsetted into a monthly history for change detection. Built upon JRC monthly water classifications, we used an enhancement algorithm developed by Zhao and Gao (2018) to map monthly SWA dynamics. This results in a better dataset (henceforth referred to as GRSAD) to overcome limitations in previous JRC datasets such as the contaminations from clouds and limitation of algorithm that classify snow and ice as non-valid observations. Analysis of JRC showed no valid data across reservoirs in January and December and pixels with no data accounted for around 23% of all pixels (contamination ratio) during 2010–2020 on average for each reservoir. This is overcome in the GRSAD approach, where over 12% of contamination pixels are repaired to construct time series. For more information, please refer to Zhao and Gao (2018). Using the reservoir shapefiles, the GRSAD algorithm is executed within the masked area to construct time series during 2010–2020. However, these shapefiles were derived from the static SRTM DEM dataset, and may represent a storage empty state with smaller extent. This problem can be addressed by buffering a specified distance outward from the shapefile to capture all valid water area changes of the reservoir. However, there are tradeoffs between large and small distances because the continual

https://doi.org/10.5194/essd-2021-470
Preprint. Discussion started: 16 May 2022

increase in water area with buffer distance could indicate either very large increases in water area beyond static reservoir shapefile or capture of non-target reservoir waters. To determine the optimal buffer size, we used five distances (30, 60, 90, 120, and 1000 m) and approached the issue of optimal buffer distance by assessing proportional water increases with increasing sizes across reservoirs. Detailed information can be found in Fig. S1 and Text S1, and we set the 120 m to construct time series. For comparisons, we compute the SWA dynamics of reservoirs using the raw JRC datasets, and use the contamination ratio (CR) as a quality flag indicator.

2.3 Reservoir storage variation estimation

Monthly reservoir storage variation estimation is based on the A–E relationships. The monthly WSE was estimated by directly averaging all measurements within each month. Attributed to the denser and more frequent records of SWA, we selected SWA values with contaminations ratio smaller than 5% for the construction of hypsometry curve for each reservoir. The data pairs were assumed to give five hypsometric relationships (linear, power, exponential, polynomial, and logarithmic relationships). Parameters of the relationships are derived by minimizing the residual sum of squares (RSS) using an ordinary least squares (OLS) regression. The curves were compared based on their R^2 values and the one with the best performance is served as the hypsometry relationship of the reservoir. We then apply this relationship to estimate WSE from SWA for periods when WSE is unavailable and inverse the function to estimate SWA from WSE for periods when SWA is unavailable (e.g., the month with large contamination ratio). Using Eq. (3), monthly RWSC estimation are determined during 2010–2020.

$$\Delta V_t = \frac{1}{2}(WSE_t - WSE_{t-1}) \times (SWA_t + SWA_{t-1}), \quad (3)$$

In cases where reservoirs show no remarkable surface area fluctuation, hypsometric relationships between WSE and SWA would not be feasible and RWSC are determined by multiplying the difference of satellite altimetry measurements with a mean reservoir area value. The coefficient of variation (CV) from the area observations are used to express area variation normalized by mean reservoir size. The reservoirs with a CV smaller than 2% (i.e., near-invariant variable) are interpreted to be constant.

3 Results

3.1 Overview

In this study, we generated the remotely-sensed reservoir datasets for 338 Chinese reservoirs, with a total of 470.6 km^3 storage capacity (i.e., 50% reservoir capacity in China). The geographical distributions of these reservoirs are represented in Fig. 1 and their data availability and evaluation reports are shown in Fig. 2. By synthesizing information from various data sources, the remotely-sensed datasets (WSE, SWA, and RWSC) were calculated during 2010–2020. Our remotely-sensed datasets have clear patterns. Seasonal filling and emptying of reservoirs are captured very well, especially the regions where the reservoir storage are dynamic. The remotely-sensed A–E relationships were also calculated. Moreover, we provide different levels of data with an easily readable file format (Wikipedia contributors, FAIR data, 2021). For more details, please refer to Sect. 3.3.

https://doi.org/10.5194/essd-2021-470
Preprint. Discussion started: 16 May 2022

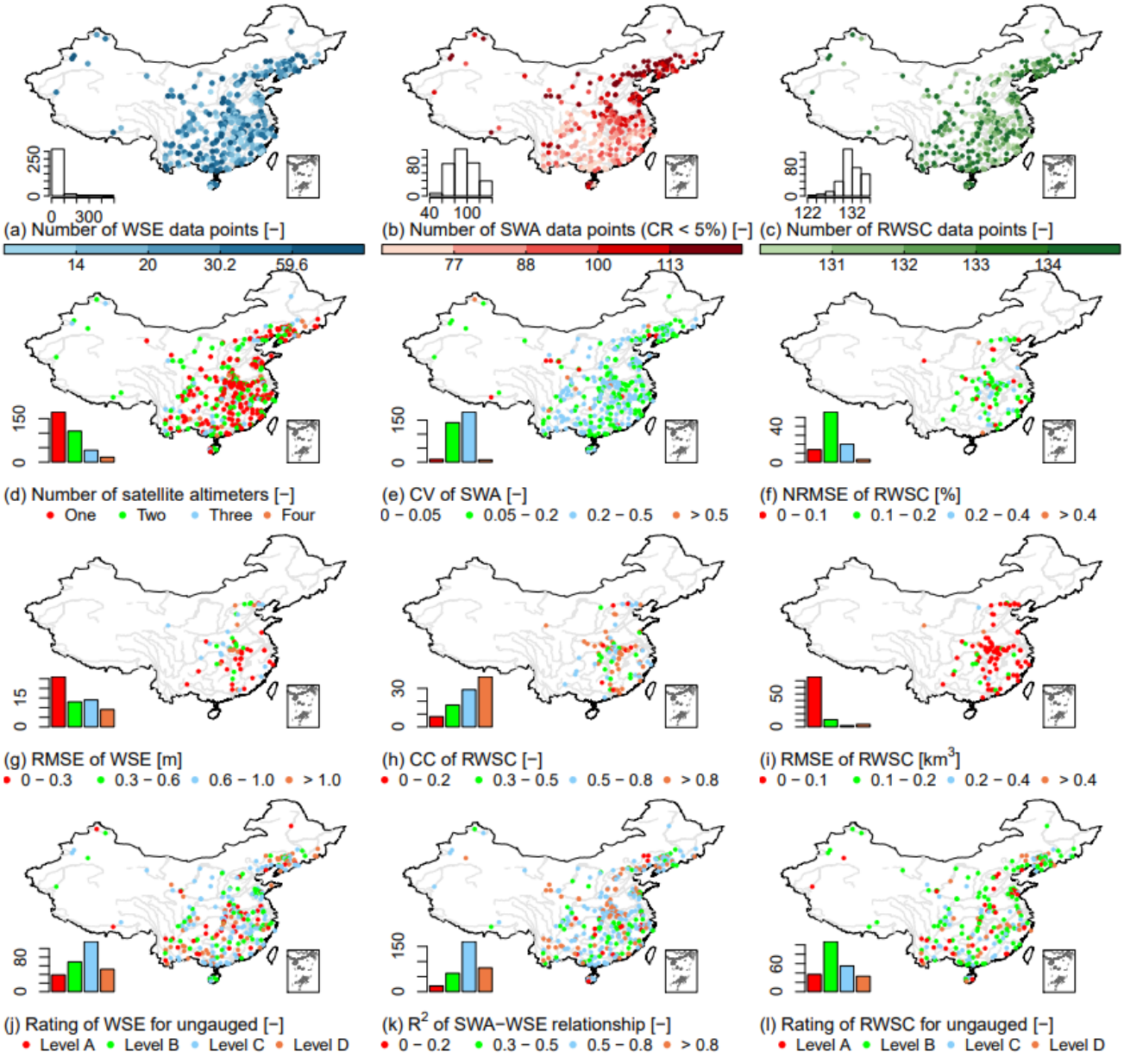

Figure 2: Overview of the remotely-sensed datasets of 338 Chinese reservoirs. The histograms indicate the number of reservoirs in each bin. Using four satellite altimeters, we merge all altimetric observations for a specific reservoir from multisource if available (d). (a) denotes the number of data points of the merged WSE data for each reservoir. For evaluation, we validate the remotely-sensed WSE of 62 reservoirs in terms of RMSE (g), and qualitatively evaluated the remaining 276 reservoirs using qualitative letter grades (j). Due to the insufficient WSE-SWA data pairs of 13 reservoirs, we obtain the monthly remotely-sensed RWSC of 325 reservoirs. For evaluation, we validate the remotely-sensed RWSC of 93 reservoirs in terms of NRMSE, RMSE, and CC (f, i, h), and qualitatively evaluated the remaining reservoirs using qualitative letter grades (l). Evaluation of the A–E relationships established by monthly WSE-SWA data pairs is performed by their R^2 of fitted curves (k) of 325 reservoirs.

https://doi.org/10.5194/essd-2021-470
Preprint. Discussion started: 16 May 2022

To evaluate the data quality, we calculate the standard deviation (SD) of WSE measurements and the contamination ratio (CR) of SWA. The SD gives a measure of how precise the observations are along each track, and the CR indicates the percentage of the pixels with no data to all pixels within the masked reservoir. Analyses showed that SD was often not an accurate predictor for WSE time-series analysis (Coss et al., 2020) Thus, we validate the remotely-sensed WSE and RWSC for 93 reservoirs with in situ observations in Sect. 3.2. Following the normal practice in the field, we compare WSE anomalies between satellites and gages by removing the mean value due to the unknown local vertical datums. Error metrics in WSE includes root-mean-square error (RMSE), and performance of RWSC is assessed by RMSE, normalized root-mean-square error (NRMSE), and Pearson correlation coefficient (CC). Performance of remotely-sensed results is considered moderate and even good based on visual inspection of time series, statistical assessment, and reported accuracies from previous publications (Villadsen et al., 2016). In the next two sections, we will show how well the remotely-sensed results are in good agreement with gauged records. For the remainder of reservoirs without in situ observations, we perform a qualitative evaluation using a letter grade (A to D, highest to lowest level of confidence on the data quality). The criteria used in the assignment of letter grades are based on the presence of obvious outliers, number of data points in the time series, and time series continuity. We perform letter grades by visual inspection and explicitly document which reservoirs are evaluated using this approach. It is worth noting that we use the most recent satellite mission from Sentinel-3 and explore how new SAR satellites may deliver reliable observations in monitoring any inland water body (the smallest reservoir with area less than 1 km^2). The close agreement between the remotely-sensed results and in situ observations provided a very good trustworthiness in the quality of our datasets, more than 75% of which show good data quality.

3.2 Evaluation

First, performance of altimetry-derived WSE over reservoirs with in-situ records is discussed. Next, comparison between in-situ and remotely-sensed RWSC is performed, followed by the qualitative performance evaluation for reservoirs without in-situ observations.

3.2.1 Validation of the remotely-sensed WSE

In total, 873 reservoirs are visited by the four altimetry missions over China during CryoSat-2 era, providing basic WSE information. After outlier's removal, time series construction and combination, and visual inspection, we finally retain 338 reservoirs that have enough valid measurements. Note that, most reservoirs are removed due to the insufficient altimetry data points rather than other reasons. Out of 338 reservoirs, most reservoirs are visited by two drifting altimeters (i.e., 225 and 118 reservoirs by CS2 and SARAL/AltiKa), while S3A/S3B covers 113/122 reservoirs, respectively (Fig. 1). Due to the missing observations of most reservoirs with in-situ records for the period of May 2018 to July 2019, we evaluate reservoirs where the overlapped WSE observations between satellites and stages are larger than 8, resulting in a total of 62 reservoirs with an average of 20 data for validation (25 by S3A, 25 by S3B, 8 by SARAL/AltiKa, 30 by CS2 and 62 by merged WSE).

https://doi.org/10.5194/essd-2021-470
Preprint. Discussion started: 16 May 2022

Open Access Earth System Science Data Discussions

Fig. 3 presents performance of four altimeters in terms of RMSE of retracked WSE with different retrackers. No significant difference is observed in terms of RMSE values among these retrackers although they are performing differently. In most cases, all retrackers retrieve WSE consistently. Interestingly, all retrackers consistently perform poorly for some reservoirs although the reservoir areas are relatively large. Appropriately, PPCOG is more robust over the most reservoirs. It should be noted that when merging WSE for a reservoir, the observations from the retracker that has the smallest RMSE are applied.

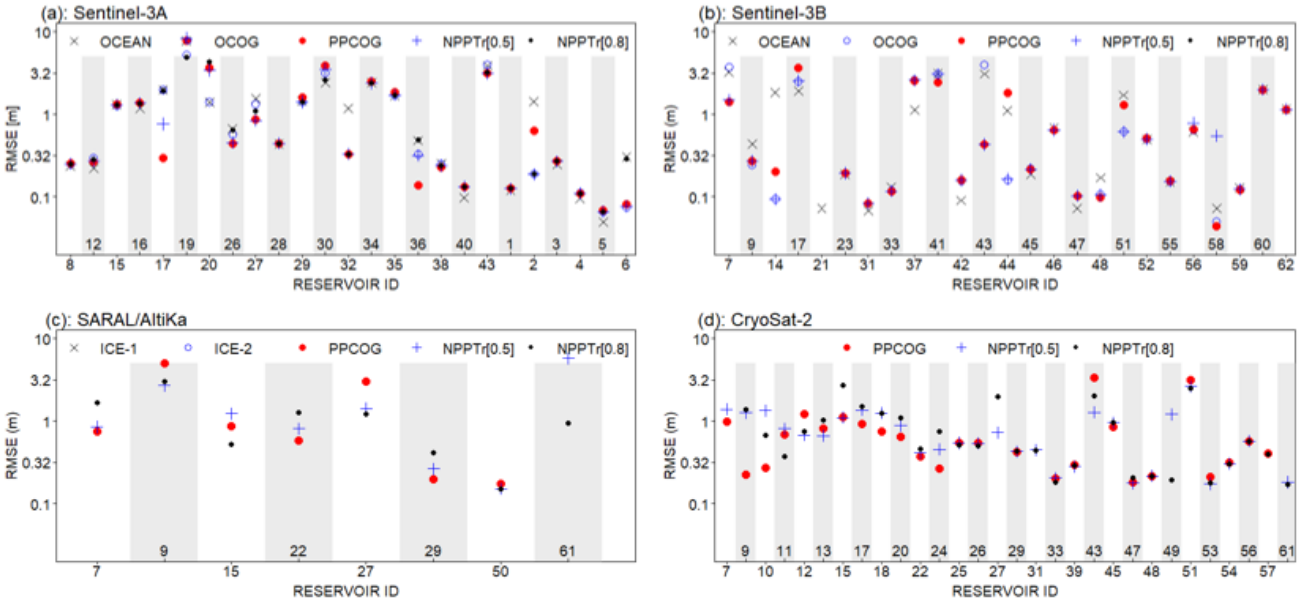

Figure 3: Comparison of the five retrackers (three for CS2) of four altimeters at validated reservoirs. Logarithmic scales are used for Y-axis. X-label refers to the reservoir IDs. For validated RESERVOIR ID, please refers to the Table S1. For some reservoirs occasionally, there is no useable data delivered by one specific retracker, and therefore no RMSE is available.

Taking the observations from the retracker that has the smallest RMSE, we merge all observations for a specific reservoir from multisource if available. Fig. 4 shows the performance of merged WSE observations in terms of RMSE values. Individually, the values of RMSE reveal that all altimetry missions can deliver useful water level measurements for reservoirs (Fig. 3). Specifically, percentages of reservoirs having very good RMSE values smaller than 0.3 m, moderate RMSE values ranging from 0.3 to 1.0 m, and relatively poor RMSE values over 1.0 m for each altimeter are 48%, 16%, 36% (S3A: validated in 25 reservoirs), 56%, 20%, 24% (S3B: 25), 38%, 50%, 12% (SARAL/AltiKa: 8), and 37%, 53%, 10% (CS2: 30), respectively. After merging observations from multisource if available, a total of 62 reservoirs are evaluated: 39 reservoirs have a good agreement with in situ data with a RMSE value below 0.6 m, among which 26 reservoirs have a very good data quality with a RMSE value smaller than 0.3 m. Another 14 reservoirs have a moderate RMSE value from 0.6 to 1.0 m. Nevertheless, around 15% has relatively poor performance in terms of RMSE values regardless of reservoir area. Some of them are located on the tributaries of the Yellow River and the Yangtze River. To demonstrate the densified water level observations from multisource if available, fifteen reservoirs intersected by different altimetry missions are shown in Fig. 5. Ideally, fifteen cases can be

https://doi.org/10.5194/essd-2021-470
Preprint. Discussion started: 16 May 2022

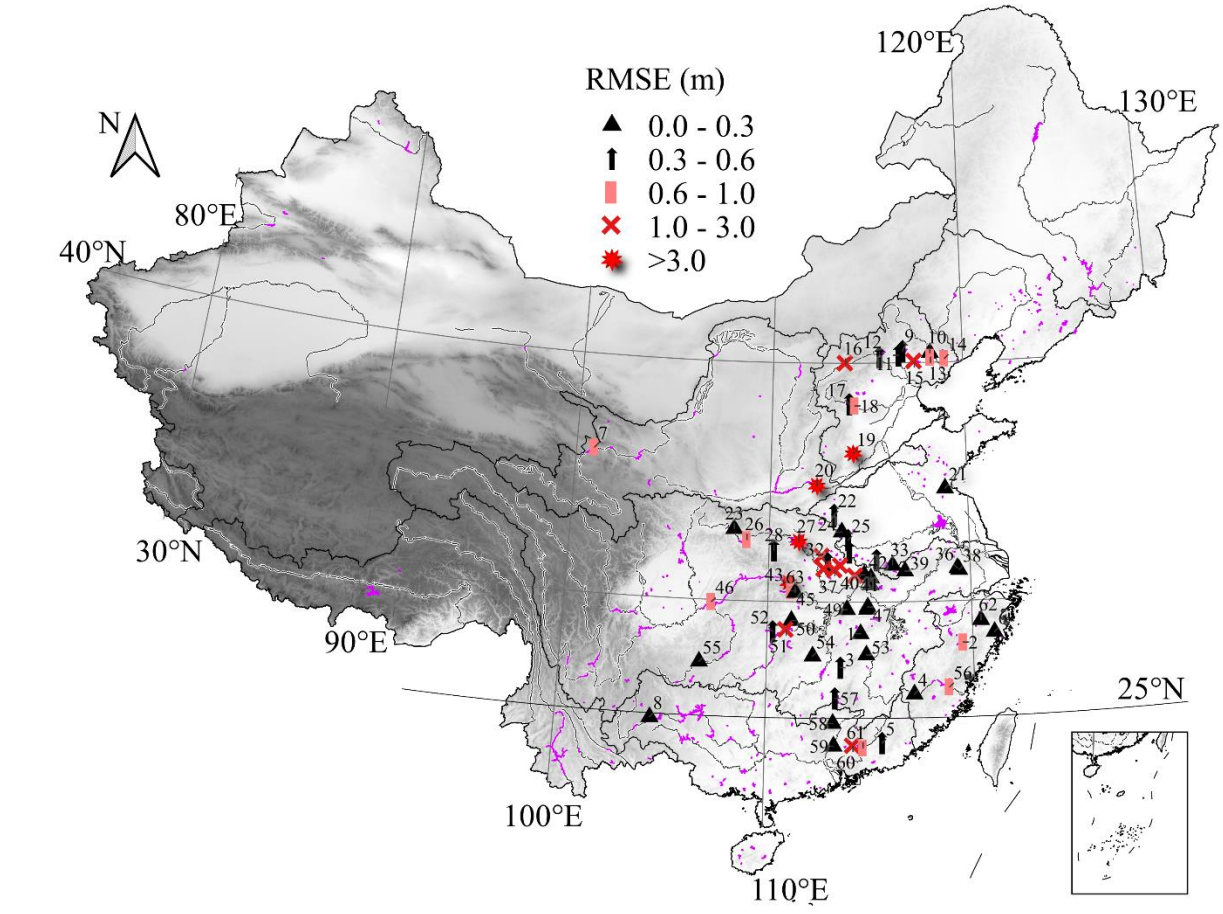

Figure 4: Performance of the merged WSE in terms of RMSE of 62 reservoirs. Note that, we merge WSE for a reservoir from multisource if available using the observations with the smallest RMSE among five (three for CS2) retracker or default PPCOG retracker. The categories are based on reported accuracy from Jiang et al., (2020). For validated RESERVOIR ID, please refers to the Table S1.

identified if observations from four altimeters are merged for a specific reservoir, i.e., four cases with single altimeter, ten cases with two altimeters, four cases with three missions and one case with all missions. and this is partly illustrated in Fig. 2(d) and Fig. 5. By taking advantage of four missions, we are able to densify WSE observations in most cases.

https://doi.org/10.5194/essd-2021-470
Preprint. Discussion started: 16 May 2022

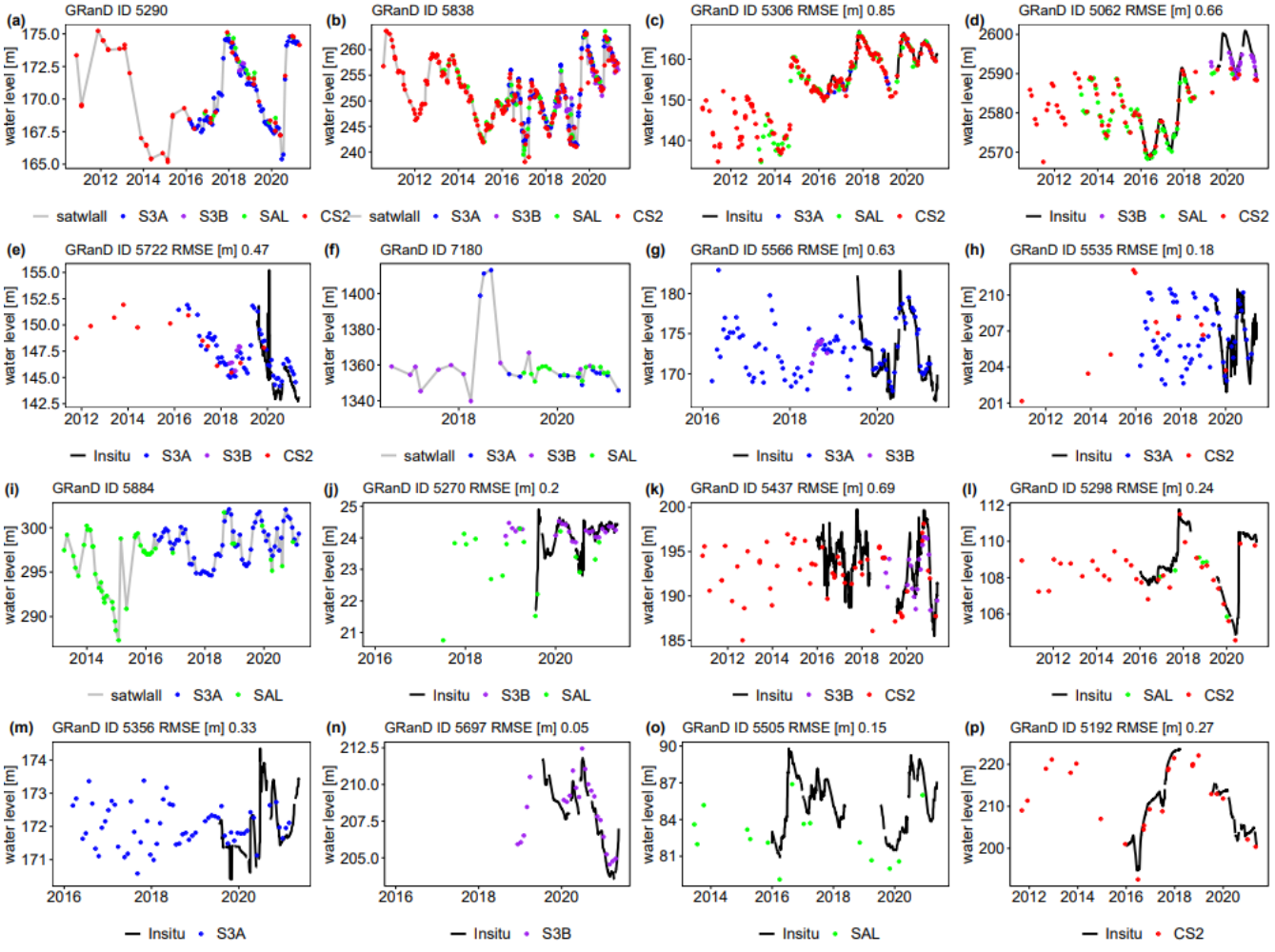

Figure 5: Illustration of merged WSE time series. Ideally, fifteen cases can be identified if four altimeters are merged for a specific reservoir, time series of merged WSE for other reservoirs are available in the datasets.

3.2.2 Validation of the remotely-sensed RWSC

The performance of remotely-send RWSC are affected by the accuracy of WSE and SWA data as well as the A–E relationships, which are firstly evaluated. Among 338 reservoirs, 13 reservoirs are excluded due to the insufficient WSE-SWA data pairs to establish the A–E relationships, thus resulting in a total of 325 reservoirs with the remotely-sensed RWSC. To evaluate the performance of SWA, we calculate CC of altimetry-derived WSE and SWA for all 325 reservoirs. Overall, time series show good agreements approximately 91% have good CC values exceeding 0.5, among which 188 reservoirs show very good agreement with a CC > 0.8 (Fig. 6). In addition, the contamination ratio is at a very low level across reservoirs and decreased by the GRSAD approach, establishing a good level of trustworthiness in SWA datasets. We notice that 62% reservoirs of A–E curves could be better explained by a second-order polynomial function, while 12% and 17% reservoirs of A–E relationships

https://doi.org/10.5194/essd-2021-470
Preprint. Discussion started: 16 May 2022

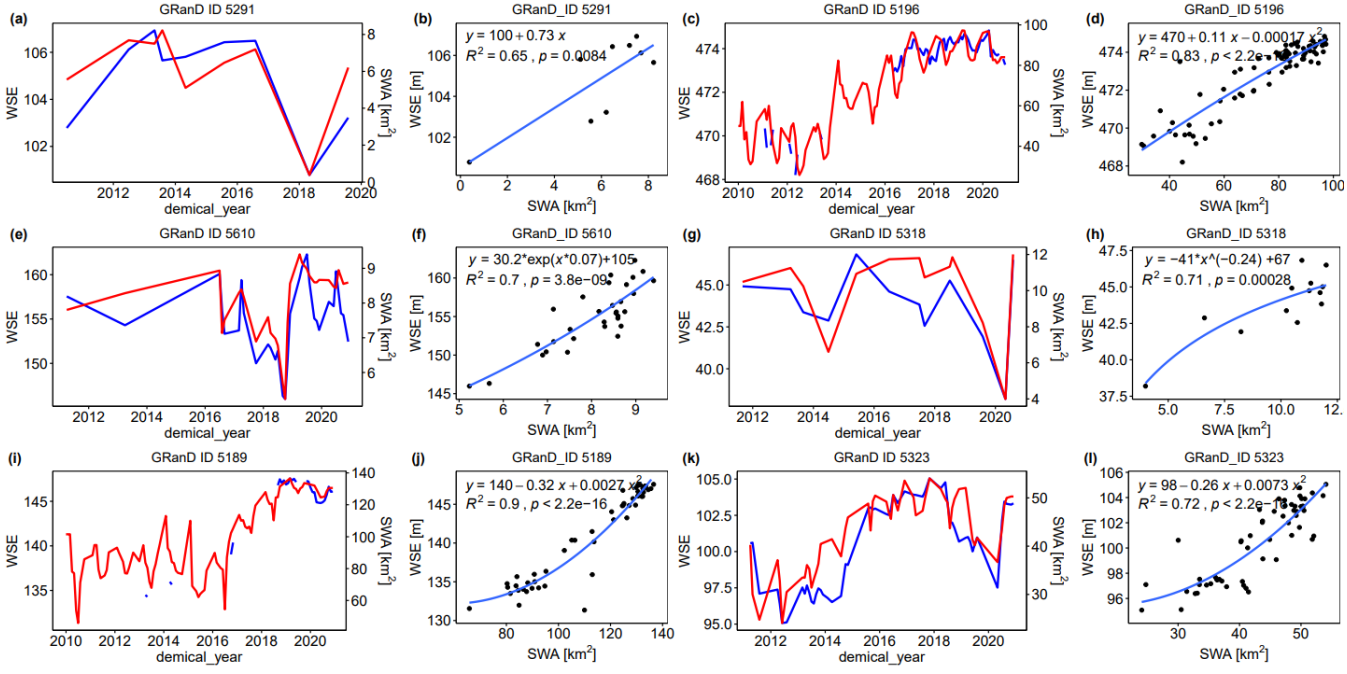

Figure 6: Illustration of time series of WSE and SWA and the associated established A–E relationships at six reservoirs. Note that: time series of WSE and SWA and associated established A–E relationships of the remaining reservoirs are available in our datasets.

are assumed to give a power and exponential function (Fig. 6 f, h). The A–E curves are evaluated based on their R^2 values (Fig. 3 k). A total of 245 of 325 reservoirs (75%) have moderate R^2 values > 0.5, among which 79 reservoirs show very good agreement with R^2 values > 0.8. Nevertheless, one fourth has relatively poor performance in terms of R^2 values. Overall, our A–E curves are reliable and lay the good foundation for RWSC estimates.

Fig. 3 (f), (i), and (h) present performance of the remotely-sensed RWSC of 93 reservoirs, and we selected 16 reservoirs here to illustrate time series of remotely-sensed RWSC (Fig. 7). Across gauge comparisons of RWSC, the median statistics of CC, NRMSE, and RMSE are 0.76, 15%, and 0.035 km^3. Around 75% reservoirs (70 of 93) show good data quality with a NRMSE value below 20% and a RMSE value ranging from 0.01 to 0.35 km3. The lowest NRMSE is 6%, from the Huanglishu reservoir that displays high CC and low RMSE values. Nonetheless, there are some differences. Some reservoirs with good NRMSE and RMSE values show poor performance in terms of CC value, e.g., the Fengtan reservoir (CC: 0.50, NRMSE: 15%, RMSE 0.14 km^3) that experiences relatively significant surface water dynamics (Fig. 7o). Closer examination in Fig. 7 seems to indicate that almost all remotely-sensed RWSC estimates show similar patterns to the observations, i.e., both positive or negative, despite of some large discrepancies when capturing peak values. Moderately poor performance of 19 reservoirs (20%) in terms of high NRMSE/RMSE and low CC values (CC < 0.4) is likely associated with their poor performances from the remotely-sensed WSE and SWA.

https://doi.org/10.5194/essd-2021-470
Preprint. Discussion started: 16 May 2022

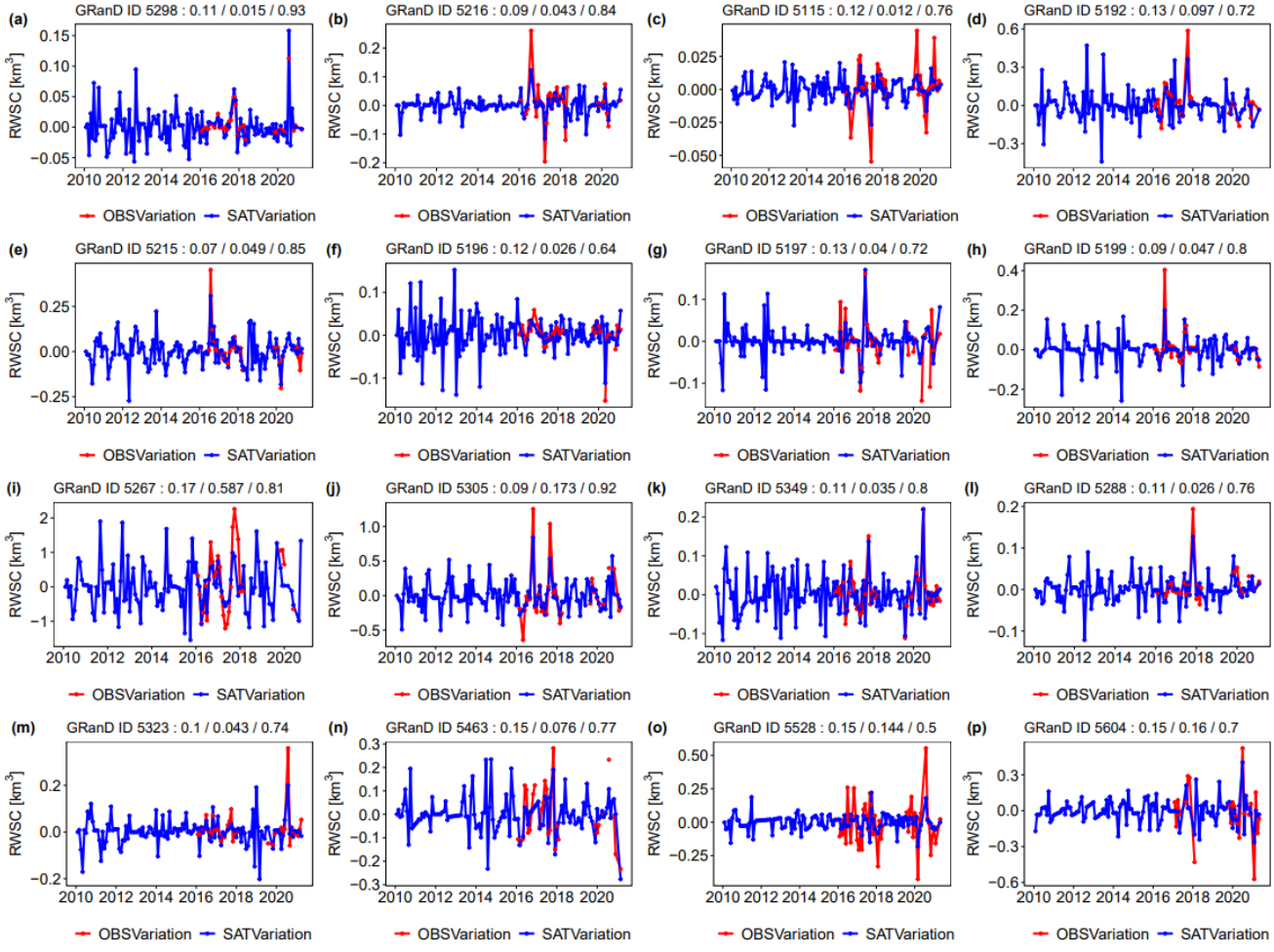

Figure 7: Illustration of time series of the remotely-sensed RWSC of 16 reservoirs. NRMSE/RMSE (km^3)/CC values are given at the top of each subplot. Note that: time series of the remotely-sensed RWSC of the remaining reservoirs (validated or not validated) are available in our datasets.

3.2.3 Qualitative performance evaluation

For 276 of 338 reservoirs, no in situ observations are available for evaluation of WSE. Note that the standard of error (SD) estimates measure the accuracy of along-track SWE at the level of single data point, it is recommended that these errors could be considered as the merged WSE datasets they are a part of. In this case, we give qualitative letter grades for 276 reservoirs. Qualitative letter grades are also determined based on the number of data points and obvious outliers in the time series, and continuity of time series. For readers a clear understanding, we select 16 representative reservoirs to illustrate their qualitative letter grades and the time series of the remotely-sensed WSE (Fig. 8). For end users, comprehensive evaluation reports and letter grades are given in the datasets. Most reservoirs get the B or C rating (approximately 67 %), with around 14% falling into the A category (Fig. 3 j). For 232 of 325 reservoirs, no in situ observations are available for evaluation of RWSC. We give

https://doi.org/10.5194/essd-2021-470
Preprint. Discussion started: 16 May 2022

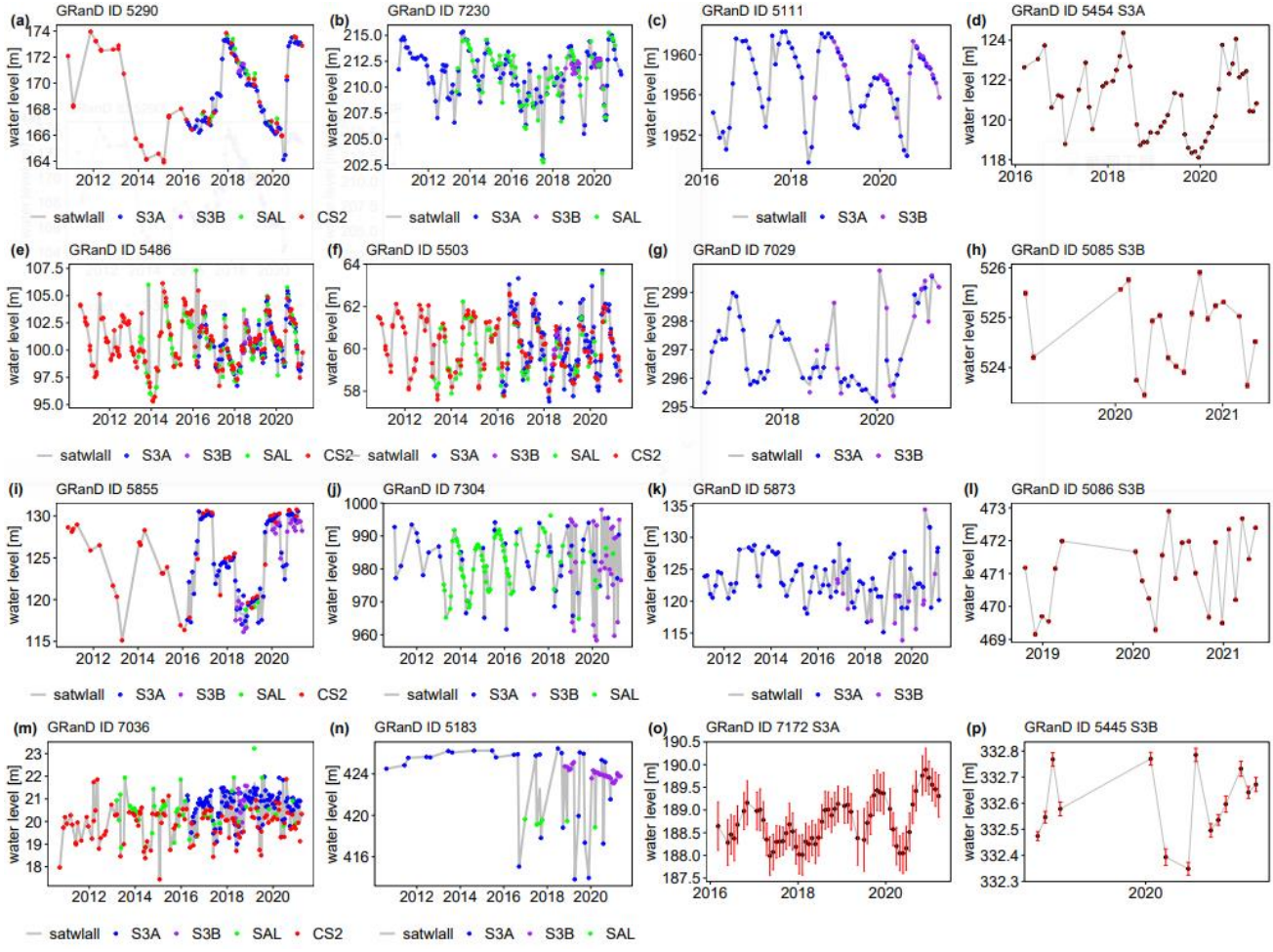

Figure 8: Illustration of qualitative letter grades of the remotely-sensed WSE of 16 reservoirs. First panel to fourth panel indicate the grade level A to D, respectively. Note that, qualitative letter grades are shown in Fig. 3 and time series of the remotely-sensed results of the remaining reservoirs are available in our datasets.

3.3 Data set description

The datasets of 338 Chinese reservoirs are publicly available at https://doi.org/10.5281/zenodo.5812012 (Shen et al., 2021). The files provided are: (i) the reservoir shapefiles, (ii) the time series of SWA, WSE and RWSC, and (iii) a readme file. In the directory of 01_res_loc, we provide two ESRI shapefiles (the location of 338 reservoirs and 93 reservoirs with in-situ observations for validation) and one Excel file of their associated attributes. In the directory of 02_res_wse, we provide the time series of reservoir water surface elevation in two modes (i.e., standard-Measurement and enhanced-Measurement), with their comprehensive evaluation reports and figures in PDF and Excel files. The standard-Measurement products are individual

https://doi.org/10.5194/essd-2021-470
Preprint. Discussion started: 16 May 2022

measurements from each satellite altimeter with different retrackers, while the enhanced-Measurement products are the densified water level observations from multisource if available. In the directory of 03_res_swa, we provide monthly area time series from 2010 to 2000 for 338 Chinese reservoirs. The directory of 04_res_rwsc contains both A–E curves and time series of RWSC for 325 reservoirs, with their comprehensive evaluation reports, regression statistics, and figures in PDFs and Excels.

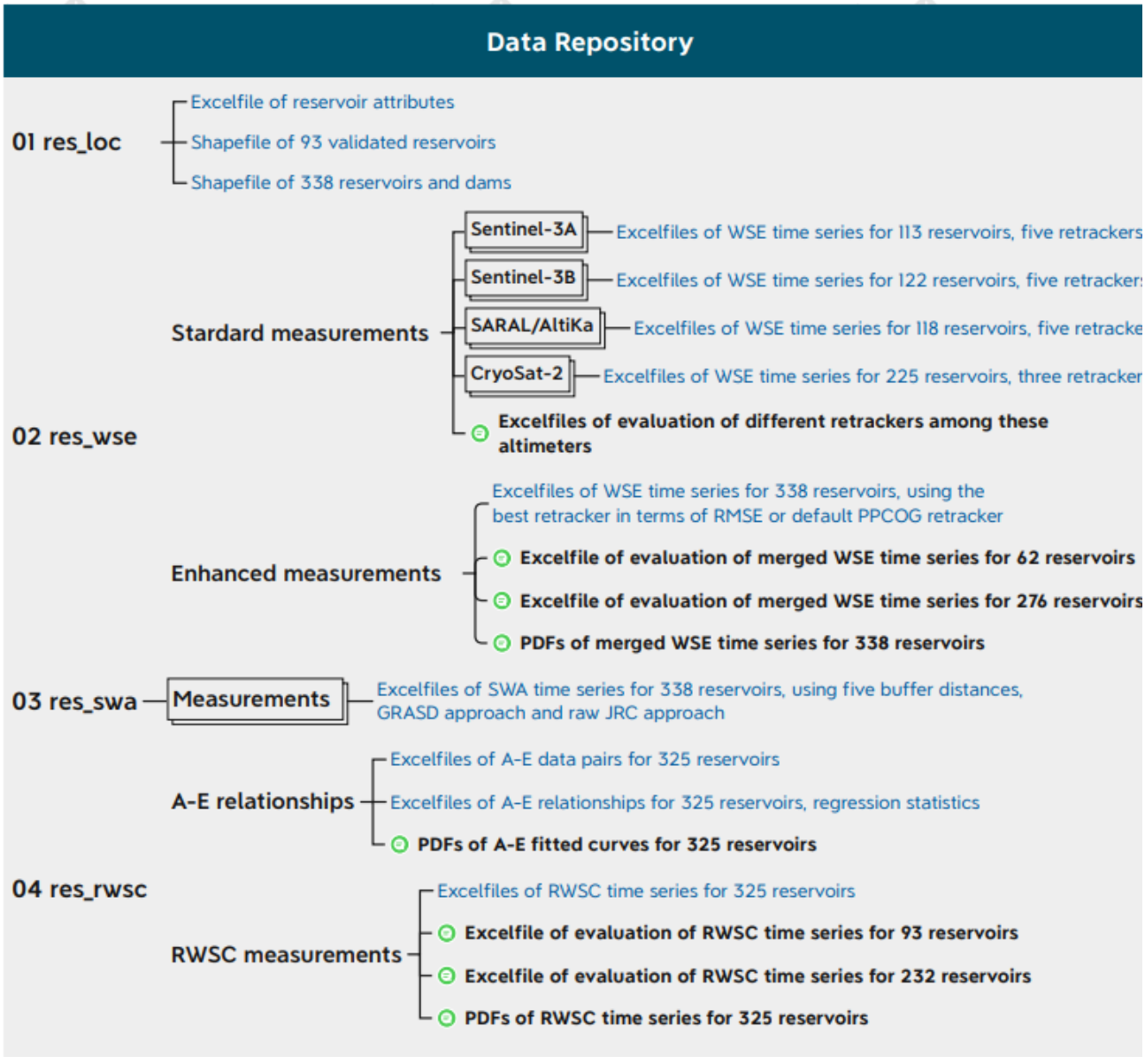

Figure 9: Folder structure of the remotely-sensed reservoir datasets. For more details, please refer to the repository.

https://doi.org/10.5194/essd-2021-470
Preprint. Discussion started: 16 May 2022

4 Discussion

4.1 Comparison to existing similar products

Note that the remotely-sensed datasets developed by previous studies discussed in the Sect. 1 are unavailable or do not match the coverage of any reservoirs in our dataset. Nonetheless, we compare 28 reservoirs of our dataset with three databases from G-REALM, DAHITI and Hydroweb and notice that our remotely-sensed dataset is comparable (Fig. 10 and Fig. A1). If in-situ observations available, the time series from different sources are compared against in situ measurements and the RMSE values are calculated, otherwise; the CC values of WSE estimates of online database and our dataset are calculated. Across 7 gage comparisons (Fig. 10 d-j), G-REALM, DAHITI, Hydroweb and our dataset are similar and show close agreement with in-situ measurements. Nonetheless, there are some differences. For the Three Gorge, Xiaolangdi, and Shiquan reservoirs (Fig. 10 d-f), our dataset can be less noisy and better represent the dynamics in water level, with lower RMSE values than other sources. In case of the other four reservoirs (Fig. 10 g-j), the RMSE values of our dataset are slightly higher than those of Hydroweb, but still fall the satisfactory results below 0.60 m. It is worth noting that the time series of our dataset are much denser than those from Hydroweb and show clearer patterns (Fig. A1). The results of 21 reservoirs without in-situ observations indicate that all time-series show dynamics of reservoir water level very well, highlighting the critical contribution of both existing and our datasets. In most cases, our dataset show good agreements with measurements from others, with CC values > 0.9. Nonetheless, there are some differences. Systematic biases are in these databases for the geoid issue (Fig. 10 j). In addition, some large discrepancies can be found in certain reservoirs, e.g., the Sanhezha reservoir (Fig. 10 c) did not show a clear fluctuation pattern as captured by G-REALM; the periods in 2020 between our dataset and Hydroweb at the Fengman reservoir (Fig. A1 d). It is worth noting that G-REALM includes the Jason altimeter with a 10-day cycle, thus, time series are much denser (Fig. 10 b). However, our datasets are denser than Hydroweb over most reservoirs (Fig. A1) and can be less noisy. These advantages would benefit the continuity and accuracy of the remotely-sensed WSE and RWSC. Overall, this section demonstrated that performance of our datasets approximates accuracy of existing global altimetry datasets.

https://doi.org/10.5194/essd-2021-470
Preprint. Discussion started: 16 May 2022

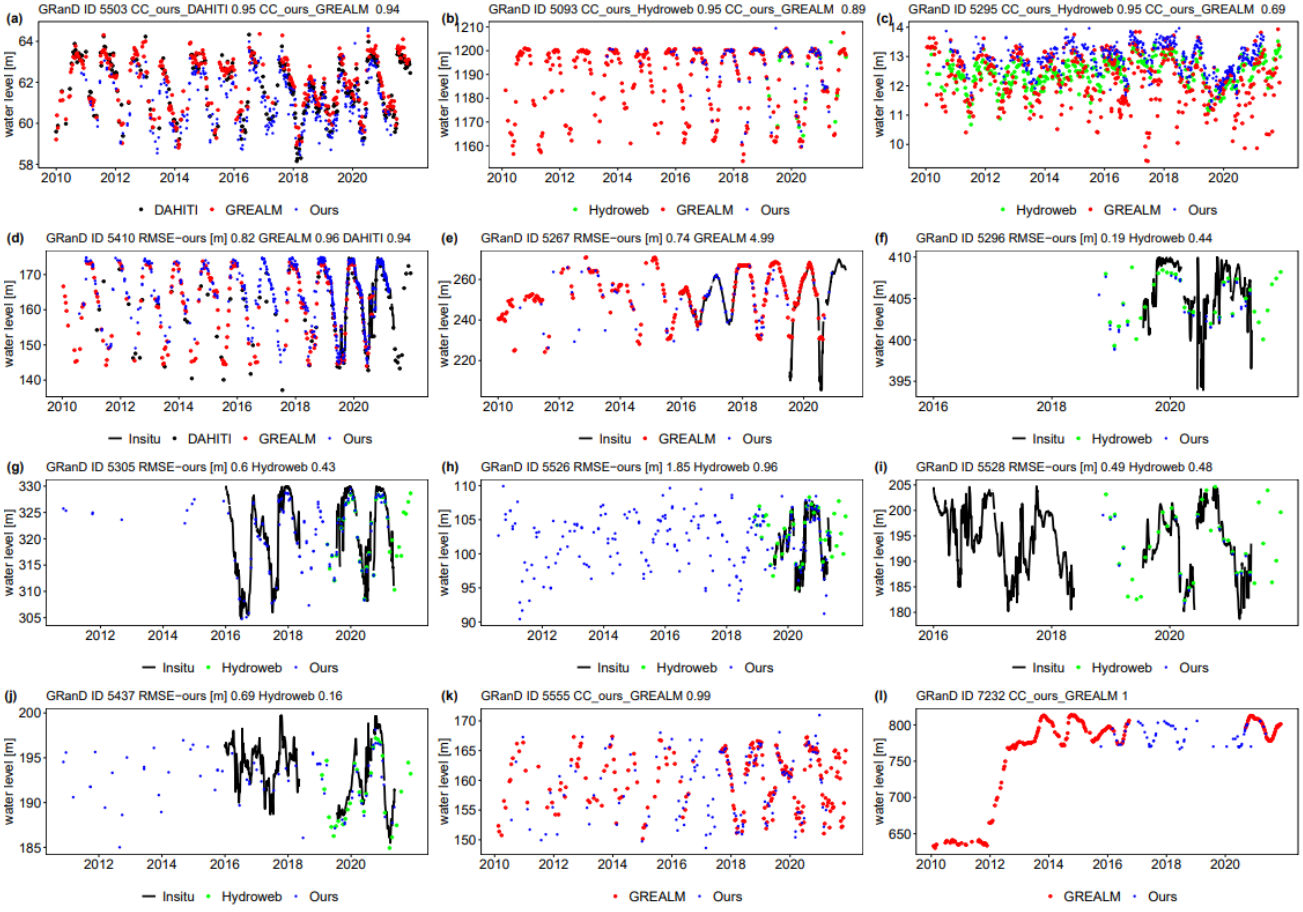

Figure 10: Multiproduct evaluation at 28 reservoirs (16 reservoirs are shown in Fig. A1). DAHITI is plotted in black, G-REALM in red, Hydroweb in green, our dataset in blue, and in-situ records in black line. RMSE values are given when in-situ observations are available, otherwise, CC values are given at the top of each subplot.

4.2 Blueprint applications

As explained earlier, our motivation is to develop the remotely-sensed reservoir datasets that can be applied as constraints to calibrate models or directly used for reservoir studies (Yigzaw et al., 2018; Shin et al., 2019, 2020). One of the most interesting scientific work that can be done with our datasets is to estimate how hydrographs in China have changed because of reservoir regulation. In order to do that, we need to combine inflow modeling with reservoir storage changes to estimate reservoir release. Fig. 11 demonstrates the flowchart of combining the process-based models or lumped models with our remotely-sensed RWSC datasets to achieve this goal. Recent studies started adopting this framework to assess the effect of dams and reservoirs on streamflow regulation, and/or downstream flood inundation (Gutenson et al., 2020; Zhong et al., 2020; Tavakoly et al., 2021). Here, following the normal but simple practices (Bonnema and Hossain 2019; Han et al., 2020), we estimate reservoir release using our remotely-sensed RWSC dataset and inflow simulated by a calibrated lumped hydrological model (i.e., GR4J, Génie Rural à 4 paramètres Journalier model), to demonstrate the potential of our datasets to help achieve this goal (Fig. 11). This

https://doi.org/10.5194/essd-2021-470
Preprint. Discussion started: 16 May 2022

experiment is carried out at the Ankang reservoir, which has a water capacity of 2.58 km^3 and a water extent of 58 km^2, located in the Han River. The basin-averaged precipitation from high quality GPM-Final products and potential evaporation are used to run the model. The Oudin approach is used to calculate the potential evaporation, and requires temperature from ERA5-Land products for calculation (Oudin et al., 2005). The model is pre-calibrated based on 10-year historical reservoir inflows (2001-2007 for calibration, 2008-2010 for validation). The Shuffled Complex Evolution (SCE-UA) is employed to calibrate the hydrological model through maximizing the Kling-Gupta Efficiency (KGE) value. Then, we simulate reservoir inflow during 2010-2020 in combination with our RWSC for release estimates. The values of KGE and streamflow hydrographs reveal that model performs well with KGE > 0.68 during both calibration and validation periods. The releases show good agreements to the observations, with KGE exceeding 0.90 and NRMSE below 0.04. Moreover, reservoir regulations on natural streamflow are nicely captured (Fig. 12 f), favoring the success of the framework and our datasets. In spite of good performance of our case study, the limitations can be seen that some reservoir variables (precipitation and evaporation) are neglected and the case study fails to provide a big picture of streamflow impacts of reservoir regulation. Acknowledging such limitations, we argue that the datasets could help achieve the blueprint application by introducing the key components (e.g., RWSC) of reservoirs at national scale.

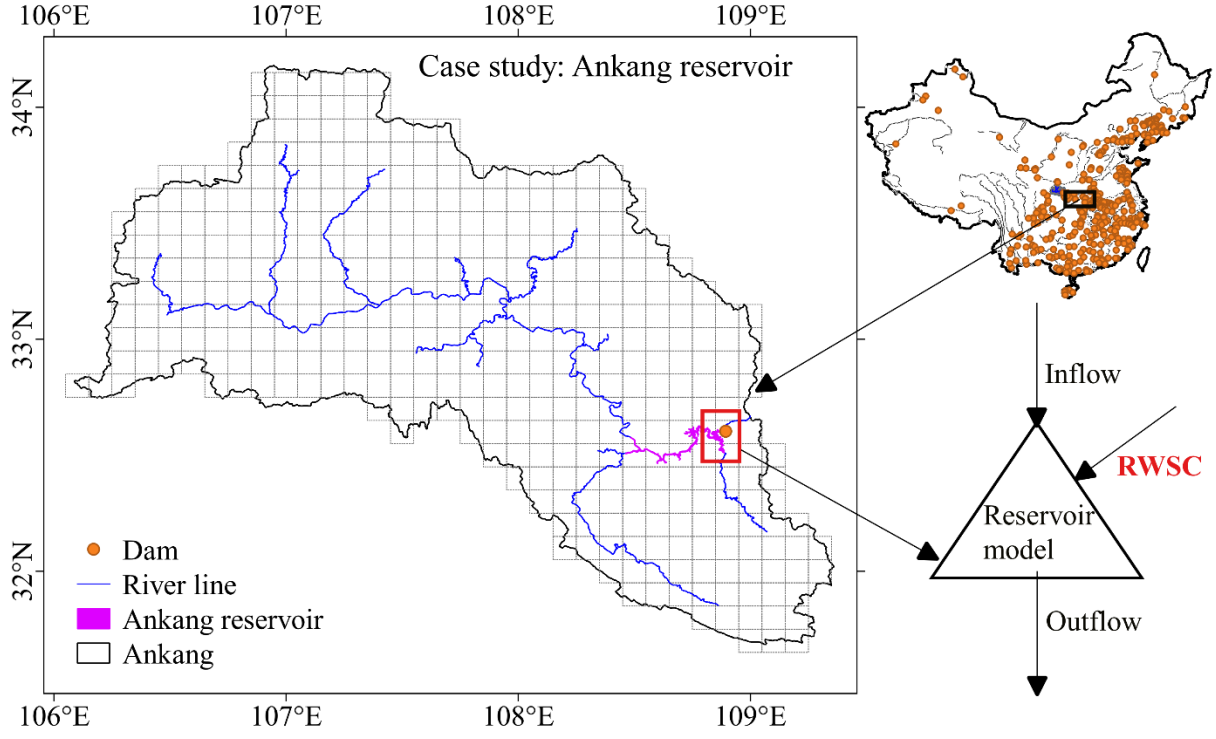

Figure 11: Schematic representation of integration between models and our datasets for reservoir release application. Normally, streamflow at the node (i.e., the dam) should be replaced with regulated flow (i.e., reservoir outflow) and routed downstream by a routing model such as RAPID model. The remotely-sensed RWSC and inflow simulated by hydrological models are introduced to the reservoir model, i.e., the mass balance equation.

https://doi.org/10.5194/essd-2021-470
Preprint. Discussion started: 16 May 2022

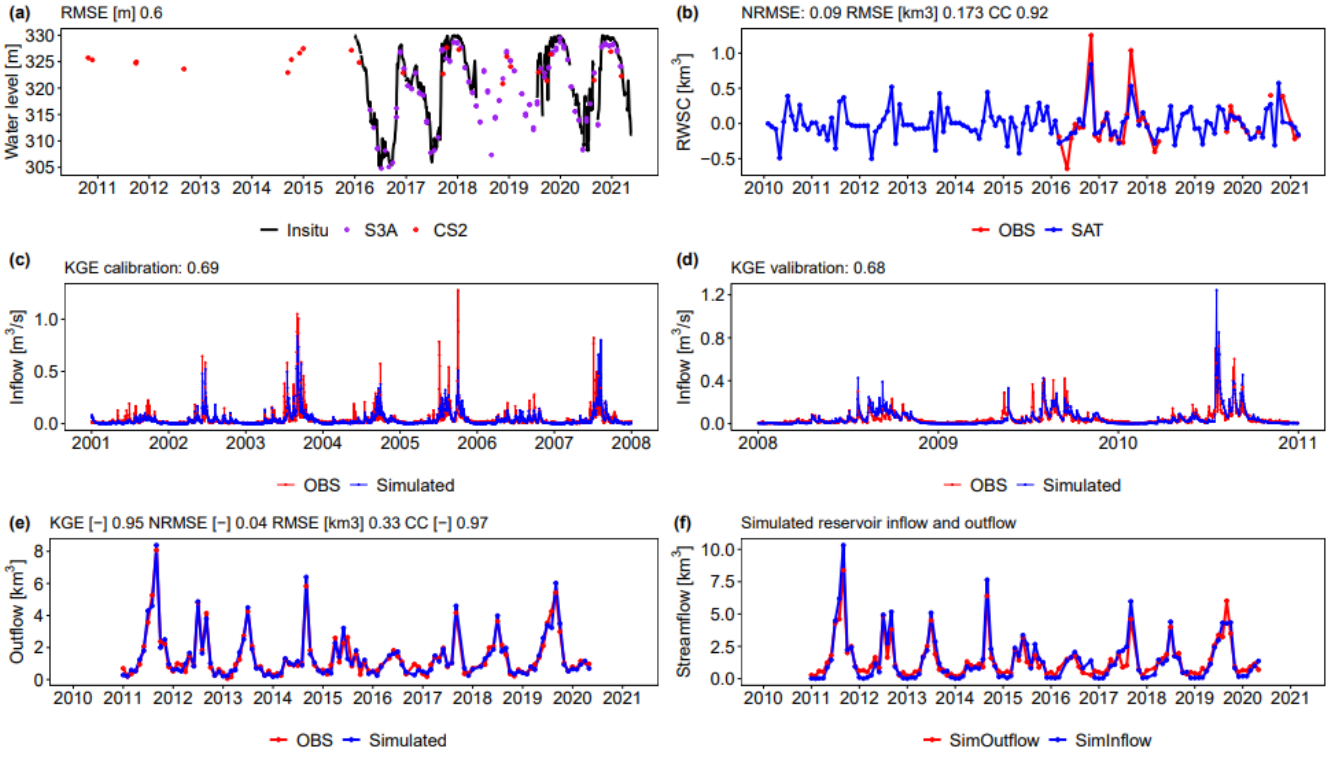

Figure 12: Case study at the Ankang reservoir. (a) and (b) are the evaluation of the remotely-sensed WSE and RWSC. (c) and (d) denote the streamflow hydrographs simulated by GR4J model during calibration and validation periods. (e) represents the comparison of model simulated outflows and gauged records. (f) shows streamflow regulation by reservoirs. Note that: only historical inflow records before 2010 are available in this study.

The datasets can benefit other applications across multiple disciplines in addition to areas described above. We highlight three areas for future applications. First, the RWSC can be used to develop a reservoir storage forecast system (Tiwari and Mishra, 2019) at 1- to 3-month lead that can be valuable for water resource management in China. Second, the datasets can be joined with hydrological and climate datasets to synthesize changes in water quantity and quality. For example, the datasets could be combined with carbon dioxide emissions from Carbon Monitor CHINA (https://cn.carbonmonitor.org/) to address questions that how changes in reservoir storage may co-vary with changes in carbon dioxide emissions. Third, the datasets can be extended to include other countries and thousands of small reservoirs, in the background of booming satellites such as the Surface Water and Ocean Topography mission that detects smaller water bodies (Biancamaria et al., 2016).

4.3 Advantages and limitations

To the authors' best knowledge, our research fills such a data gap of the remotely-sensed reservoir datasets at national scale. We use the recent satellite altimetry mission (e.g., Sentinel-3) and explore how new SAR satellite altimeters may have reliable observations for reservoirs. In total, comprehensive reservoir information for 338 major reservoirs are generated, with a total of 470.6 km^3 water storage, accounting for 50% reservoir capacity in China. More importantly, the in-situ observations of 93 reservoirs are used in this study as a critical reference to validate both the remotely-sensed WSE and RWSC, thereby bringing

https://doi.org/10.5194/essd-2021-470
Preprint. Discussion started: 16 May 2022

the highest level of confidence on data quality. Our error statistics of RWSC are slightly higher than previous studies in terms of NRMSE ranging from 5% to 20% (Han et al., 2020; Zhong et el., 2020). This discrepancy is likely because we include a wide range of reservoirs where evaluations have not been conducted in the previous publications and because we do not fine-tune process or filter each reservoir due to the national scale of the dataset. Nevertheless, over 75% reservoirs evaluated by in-situ observations fall into the good category showing NRMSE values of RWSC below 20%. This dataset also contributes a knowledge with regard to performances of current four operational altimeters in monitoring reservoir water level. More than 85% reservoirs evaluated by in-situ observations fall into the good category showing RMSE values of WSE retracked by these four altimeters below 1.0 m. Nonetheless, more general algorithms with better performance regardless of the reservoir's attributes and the data with higher temporal resolution (e.g. Jason altimetry missions) will be our next studies.

5 Conclusions

In this study, we utilize four satellite altimetry missions from SARAL/AltiKa, Sentinel-3 A/B, and CroySat-2 in combination with Landsat-based optical water datasets (GRSAD), to develop high-resolution reservoir datasets of WSE, SWA, and RWSC. The resulting datasets include 338 reservoirs with a total of 470.6 km^3 water storage accounting for 50% reservoir capacity in China. The remotely-sensed results are validated against gauged measurements of 93 reservoirs: (1) The comparisons indicate the relatively high reliability and accuracy of monthly RWSC estimations, with 75% reservoirs (70 of 93) having good RMSE values from 0.002 km^3 to 0.35 km^3 and NRMSE values < 20%. For RWSC, the median statistics of CC, NRMSE, and RMSE are 0.76, 15%, and 0.035 km^3. (2) Satisfactory results and good agreements can be found between the WSE retracked by four altimeters and gauges. Individually, the percentages of reservoirs having good data quality with RMSE values below 0.3 m, moderate RMSE values from 0.3 to 1.0 m, and relatively poor RMSE values over 1.0 m for each altimeter are 48%, 16%, 36% (S3A: validated in 25 reservoirs), 56%, 20%, 24% (S3B: 25), 38%, 50%, 12% (SARAL/AltiKa: 8), and 37%, 53%, 10% (CS2: 30), respectively. After merging WSE observations from multisource if available, a total of 53 of 62 (85%) reservoirs have good and moderate data quality with a RMSE value below 1.0 m, among which 39 reservoirs show good RMSE values below 0.6 m and 26 reservoirs show very good RMSE values < 0.3 m. By taking advantage of four missions, we are able to densify WSE observations in most cases. More importantly, this dataset can be immediately applied to some scientific areas described in Sect. 4.2. Overall, our study fills such a data gap by incorporating various satellites into a comprehensive reservoir data set at national scale and provides strong support for many aspects such as hydrological processes and water management studies.

6 Data availability

All the generated remotely-sensed reservoir datasets are archived and available at https://doi.org/10.5281/zenodo.5812012 (Shen et al., 2021). They are distributed with a CC-BY license.

https://doi.org/10.5194/essd-2021-470
Preprint. Discussion started: 16 May 2022

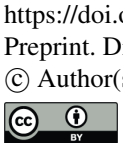

Open Access Earth System Science Data Discussions

Supplements.

The supplement related to this article is available online.

Appendix A.

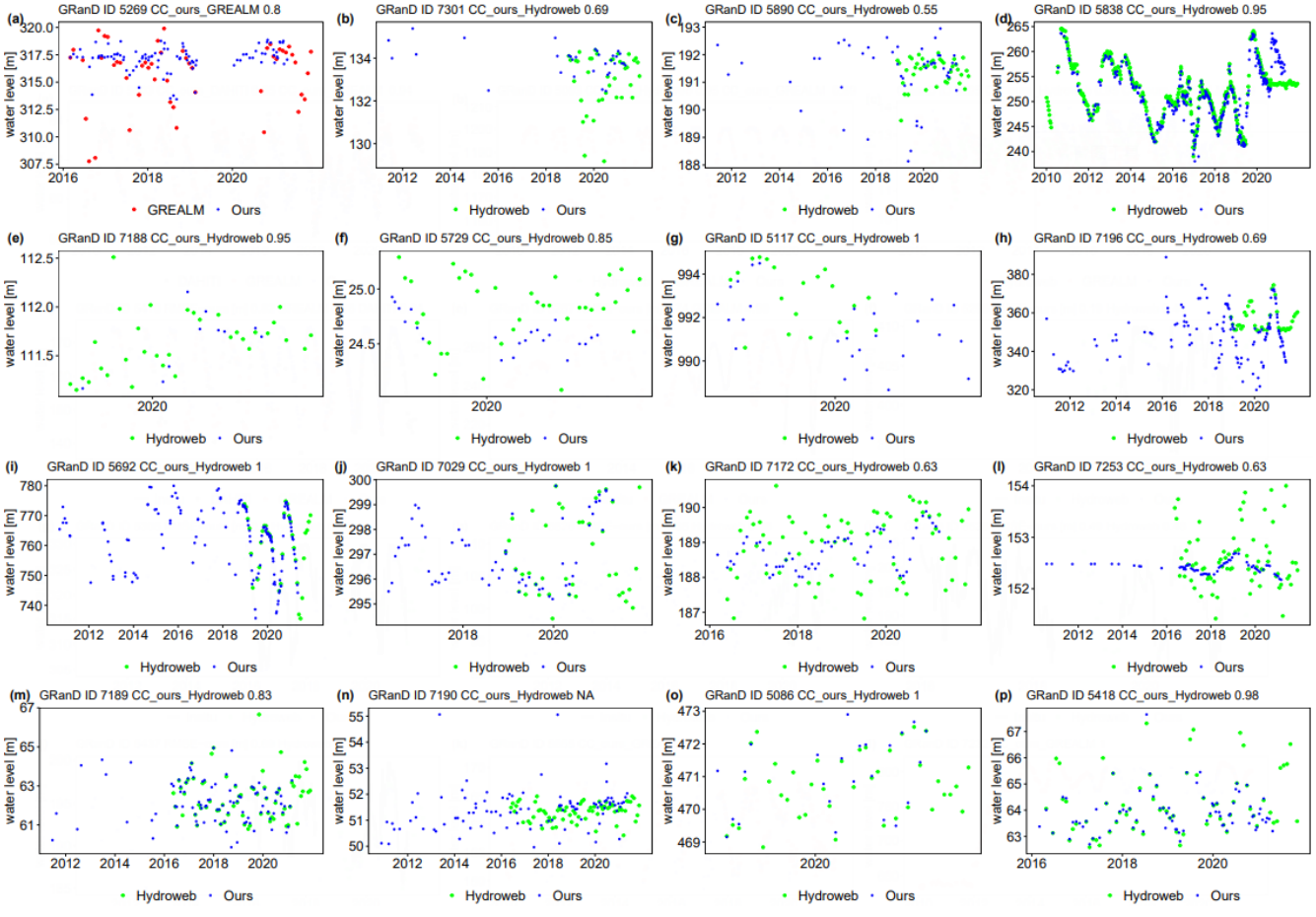

Fig. A1: Multiproduct evaluation at 16 reservoirs. DAHITI is plotted in black, G-REALM in red, Hydroweb in green, our dataset in blue, and in-situ records in black line. RMSE values are given when in-situ observations are available, otherwise, CC values are given at the top of each subplot.

Author contributions.

Y.S. and D.L. initiated the investigation. Y.S., D.L., L.J., and J.Y. designed the research. Y.S. processed the data and created the figures. K.N. initially extracted and processed the altimetry data. Y.S. prepared the manuscript with contributions from all co-authors.

https://doi.org/10.5194/essd-2021-470
Preprint. Discussion started: 16 May 2022

Open Access Earth System Science Data Discussions

Competing interests.

The authors declare that they have no conflict of interest.

Acknowledgements.

The authors acknowledge following data centers for providing original data:

- CryoSat-2 data: The baseline C level 1b dataset are from ESA (https://science-pds.cryosat.esa.int/)
- SARAL/AltiKa data from CNES AVISO+ (ftp://avisoftp.cnes.fr/AVISO/pub/)
- Reservoir and dam data from the GRanD (http://globaldamwatch.org/grand/) database
- Sentinel-3 level 2 data from Copernicus Open Access Hub (https://scihub.copernicus.eu/dhus/)
- Daily water level and storage data for 93 reservoirs from the local watershed agency (http://xxfb.mwr.cn/index.html) and National Hydrological Information Centre (http://113.57.190.228:8001/web/Report/BigMSKReport)
- Joint Research Centre Global Surface Water Dataset version 1.3 available at https://global-surface-water.appspot.com/

Financial supports.

This research has been funded by the National Natural Science Foundation of China (grant nos. 51579183 and 51879194) and the Danida Fellowship Centre (grant no. 18-M01-DTU).

References

Avisse, N., Tilmant, A., Müller, M. F., and Zhang, H.: Monitoring small reservoirs' storage with satellite remote sensing in inaccessible areas, Hydrol. Earth Syst. Sci., 21, 6445–6459, doi: 10.5194/hess-21-6445-2017, 2017.

Biancamaria, S., Lettenmaier, D. P., and Pavelsky, T. M.: The SWOT mission and its capabilities for land hydrology, Surv. Geophys., 37, 307–337, doi: 10.1007/s10712-015-9346-y, 2016.

Birkett, C., Reynolds, C., Beckley, B., and Doorn, B.: From research to operations: the USDA global reservoir and lake monitor, In: Coastal Altimetry. Springer, Berlin, Heidelberg, 19–50, doi: 10.1007/978-3-642-12796-0_2, 2011.

Bonnema, M., and Hossain, F.: Assessing the potential of the Surface Water and Ocean Topography Mission for reservoir monitoring in the Mekong River basin, Water Resour. Res., 55, 444–461, doi: 10.1029/2018WR023743, 2019.

Bonnema, M., Sikder, S., Miao, Y., Chen, X., Hossain, F., Pervin, I. A., Mahbubur Rahman, S. M., and Lee, H.: Understanding satellite-based monthly-to-seasonal reservoir outflow estimation as a function of hydrologic controls, Water Resour. Res., 52, 4095–4115, doi: 10.1002/2015WR017830, 2016.

Boulange, J., Hanasaki, N., Yamazaki, D., Pokhrel, Y.: Role of dams in reducing global flood exposure under climate change, Nat. Commun., 12, 1–7, doi: 10.1038/s41467-020-20704-0, 2021.

https://doi.org/10.5194/essd-2021-470
Preprint. Discussion started: 16 May 2022

Buccola, N. L., Risley, J. C., and Rounds, S. A.: Simulating future water temperatures in the north Santiam River, Oregon, J. Hydrol., 535, 318–330, doi: 10.1016/j.jhydrol.2016.01.062, 2016.

Busker, T., de Roo, A., Gelati, E., Schwatke, C., Adamovic, M., Bisselink, B., Pekel, J.-F., and Cottam, A.: A global lake and reservoir volume analysis using a surface water dataset and satellite altimetry, Hydrol. Earth Syst. Sci., 23, 669–690, doi: 10.5194/hess-23-669-2019, 2019.

Chaudhari, S., Felfelani, F., Shin, S., and Pokhrel, Y.: Climate and anthropogenic contributions to the desiccation of the second largest saline lake in the twentieth century, J. Hydrol., 560, 342–353, doi: 10.1016/j.jhydrol.2018.03.034, 2018.

CNES, SARAL/AltiKa Products Handbook, available at: https://www.aviso.altimetry.fr/fileadmin/documents/data/tools/SARAL_Altika_products_handbook.pdf, (last access: 17 December 2021), 2016.

Coss, S., Durand, M., Yi, Y., Jia, Y., Guo, Q., Tuozzolo, S., Shum, C. K., Allen, G. H., Calmant, S., and Pavelsky, T.: Global River Radar Altimetry Time Series (GRRATS): new river elevation earth science data records for the hydrologic community, Earth Syst. Sci. Data, 12, 137–150, doi: 10.5194/essd-12-137-2020, 2020.

Crétaux, J.-F., Jelinski, W., Calmant, S., Kouraev, A., Vuglinski, V., Bergé-Nguyen, M., Gennero, M.-C., Nino, F., Del Rio, R. A., Cazenave, A., and Maisongrande, P.: SOLS: a lake database to monitor in the Near Real Time water level and storage variations from remote sensing data, Adv. Space Res., 47, 1497–1507, doi: 10.1016/j.asr.2011.01.004, 2011.

Dang, T. D., Chowdhury, A. F. M. K., and Galelli, S.: On the representation of water reservoir storage and operations in large-scale hydrological models: implications on model parameterization and climate change impact assessments, Hydrol. Earth Syst. Sci., 24, 397–416, doi: 10.5194/hess-24-397-2020, 2020.

Dinardo, S., Fenoglio-Marc, L., Buchhaupt, C., Becker, M., Scharroo, R., Fernandes, M. J., Benveniste, J.: Coastal SAR and PLRM altimetry in German Bight and West Baltic Sea, Adv. Space Res., 62, 1371–1404, doi: 10.1016/j.asr.2017.12.018, 2018.

Donlon, C., Berruti, B., Buongiorno, A., Ferreira, M.-H., Féménias, P., Frerick, J., Goryl, P., Klein, U., Laur, H., Mavrocordatos, C., Nieke, J., Rebhan, H., Seitz, B., Stroede, J., and Sciarra, R.: The Global Monitoring for Environment and Security (GMES) Sentinel-3 mission, Remote Sens. Environ., 120, 37–57, doi: 10.1016/j.rse.2011.07.024, 2012.

Duan, Z., and Bastiaanssen, W. G. M.: Estimating water volume variations in lakes and reservoirs from four operational satellite altimetry databases and satellite imagery data, Remote Sens. Environ., 134, 403–416, doi: 10.1016/j.rse.2013.03.010, 2013.

European Space Agency, Mullar Space Science Laboratory, CryoSat Product Handbook, available at: https://earth.esa.int/documents/10174/125272/CryoSat-Baseline-D-Product-Handbook, (last access: 17 December 2021), 2012.

Fang, Y., Li, H., Wan, W., Zhu, S., Wang, Z., Hong, Y., and Wang, H.: Assessment of water storage change in China's lakes and reservoirs over the last three decades, Remote Sens., 11, 1467, doi: 10.3390/rs11121467, 2019.

Gao, H., Birkett, C., and Lettenmaier, D. P.: Global monitoring of large reservoir storage from satellite remote sensing, Water Resour. Res., 48, W09504, doi: 10.1029/2012WR012063, 2012.

https://doi.org/10.5194/essd-2021-470
Preprint. Discussion started: 16 May 2022

Getirana, A., Jung, H. C., and Tseng, K.-H.: Deriving three dimensional reservoir bathymetry from multi-satellite datasets, Remote Sens. Environ., 217, 366–374, doi: 10.1016/j.rse.2018.08.030, 2018.

Goumehei, E., Tolpekin, V., Stein, A., and Yan, W.: Surface water body detection in polarimetric SAR data using contextual complex wishart classification, Water Resour. Res., 55, 7047–7059, doi: 10.1029/2019WR025192, 2019.

Gutenson, J. L., Tavakoly, A. A., Wahl, M. D., and Follum, M. L.: Comparison of generalized non-data-driven lake and reservoir routing models for global-scale hydrologic forecasting of reservoir outflow at diurnal time steps, Hydrol. Earth Syst. Sci., 24, 2711–2729, doi: 10.5194/hess-24-2711-2020, 2020.

Han, Z., Long, D., Huang, Q., Li, X., Zhao, F., and Wang, J.: Improving reservoir outflow estimation for ungauged basins using satellite observations and a hydrological model, Water Resour. Res., 56, e2020WR027590, doi: 10.1029/2020WR027590, 2020.

Intralawan, A., Wood, D., Frankel, R., Costanza, R., and Kubiszewski, I.: Tradeoff analysis between electricity generation and ecosystem services in the lower Mekong Basin, Ecosyst. Serv., 30, 27–35, doi: 10.1016/j.ecoser.2018.01.007, 2018.

Jain, M., Andersen, O. B., Dall, J., and Stenseng, L.: Sea surface height determination in the Arctic using Cryosat-2 SAR data from primary peak empirical retrackers, Adv. Space Res., 55, 40–50, doi: /10.1016/j.asr.2014.09.006, 2015.

Jiang, L., Andersen, O. B., Nielsen, K., Zhang, G., and Bauer-Gottwein, P.: Influence of local geoid variation on water surface elevation estimates derived from multi-mission altimetry for Lake Namco, Remote Sens. Environ., 221, 65–79, doi: 10.1016/j.rse.2018.11.004, 2019.

Jiang, L., Nielsen, K., Dinardo, S., Andersen, O. B., and Bauer-Gottwein, P.: Evaluation of Sentinel-3 SRAL SAR altimetry over Chinese rivers, Remote Sens. Environ., 237, 111546, doi: 10.1016/j.rse.2019.111546, 2020.

Khandelwal, A., Karpatne, A., Marlier, M. E., Kim, J., Lettenmaier, D. P., and Kumar, V.: An approach for global monitoring of surface water extent variations in reservoirs using MODIS data, Remote Sens. Environ., 202, 113–128, doi: 10.1016/j.rse.2017.05.039, 2017.

Lehner, B., Liermann, C. R., Revenga, C., Vörösmarty, C., Fekete, B., Crouzet, P., Döll, P., Endejan, M., Frenken, K., Magome, J., Nilsson, C., Robertson, J. C., Rödel, R., Sindorf, N., and Wisseret, D.: High-resolution mapping of the world's reservoirs and dams for sustainable river-flow management, Front. Ecol. Environ., 9, 494–502, doi: 10.1890/100125, 2011.

Li, Y., Gao, H., Zhao, G., and Tseng, K. H.: A high-resolution bathymetry dataset for global reservoirs using multi-source satellite imagery and altimetry, Remote Sens. Environ., 244, 111831, doi: 10.1016/j.rse.2020.111831, 2020.

Liu, J., Jiang, L., Zhang, X., Druce, D., Kittel, C. M. M., Tøttrup, C., and Bauer-Gottwein, P.: Impacts of water resources management on land water storage in the North China Plain: Insights from multi-mission earth observations, J. Hydrol., 603, 126933, doi: 10.1016/j.jhydrol.2021.126933, 2021.

Marx, A., Dusek, J., Jankovec, J., Sanda, M., Vogel, T., van Geldern, R., Hartmann, J., and Barth, J. A. C.: A review of CO2 and associated carbon dynamics in headwater streams: A global perspective, Rev. Geophys., 55, 560–585, doi: 10.1002/2016RG000547, 2017.

Mu, M., Tang, Q., Han, S., Liu, X., and Cui, H.: Using GRanD database and surface water data to constrain area–storage curve of reservoirs. Water, 12, 1242, doi: 10.3390/w12051242, 2020.

Nielsen, K., Stenseng, L., Andersen, O. B., Villadsen, H., and Knudsen, P.: Validation of CryoSat-2 SAR mode based lake levels, Remote Sens. Environ., 171, 162–170, doi: 10.1016/j.rse.2015.10.023, 2015.

Oudin, L., Hervieu, F., Michel, C. Perrin, C., Andréassian, V., Anctil, F., and Loumagne, C.: Which potential evapotranspiration input for a lumped rainfall-runoff model? Part 2-Towards a simple and efficient potential evapotranspiration model for rainfall-runoff modelling, J. Hydrol., 303, 290–306, doi: 10.1016/j.jhydrol.2004.08.026, 2005.

Pavlis, N. K., Holmes, S. A., Kenyon, S. C., and Factor, J. K.: The development and evaluation of the Earth Gravitational Model 2008 (EGM2008), J. Geophys. Res. Solid Earth, 117, doi: 10.1029/2011JB008916, 2012.

Pokhrel, Y., Shin, S., Lin, Z., Yamazaki, D., and Qi, J.: Potential disruption of flood dynamics in the lower Mekong River Basin Due to upstream flow regulation, Sci. Rep., 8, 1–13, doi: 10.1038/s41598-018-35823-4, 2018.

Schwatke, C., Dettmering, D., Bosch, W., and Seitz, F.: DAHITI – an innovative approach for estimating water level time series over inland waters using multi-mission satellite altimetry, Hydrol. Earth Syst. Sci., 19, 4345–4364, doi: 10.5194/hess-194345-2015, 2015.

Shen, Y., Liu, D., Jiang, L., Nielsen, K., Yin, J., Liu, J., and Bauer-Gottwein, P.: Data of essd-2021-470, Zenodo [data set], doi: 10.5281/zenodo.5812012, 2021.

Shen, Y., Liu, D., Jiang, L., Tøttrup, C., Druce, D., Yin, J., Nielsen, K., Bauer-Gottwein, P., Wang, J., and Zhao X.: Estimating reservoir release using multi-source satellite datasets and hydrological modeling techniques, Remote Sens., 14, 815, doi: 10.3390/rs14040815, 2022.

Shin, S., Pokhrel, Y., and Miguez-Macho, G.: High-resolution modeling of reservoir release and storage dynamics at the continental scale, Water Resour. Res., 55, 787–810, doi: 10.1029/2018WR023025, 2019.

Shin, S., Pokhrel, Y., Yamazaki, D., Huang, X., Torbick, N., Qi, J., Pattanakiat, S., Ngo-Duc, T., and Nguyen, T. D.: High resolution modeling of river-floodplain-reservoir inundation dynamics in the Mekong River Basin, Water Resour. Res., 56, e2019WR026449, doi: 10.1029/2019wr026449, 2020.

Shu, S., Liu, H., Beck, R. A., Frappart, F., Korhonen, J., Lan, M., Xu, M., Yang, B., and Huang, Y.: Evaluation of historic and operational satellite radar altimetry missions for constructing consistent long-term lake water level records, Hydrol. Earth Syst. Sci., 25, 1643–1670, doi: 10.5194/hess-25-1643-2021, 2021.

Song, C., Huang, B., and Ke, L.: Modeling and analysis of lake water storage changes on the Tibetan Plateau using multi-mission satellite data, Remote Sens. Environ., 135, 25–35, doi: 10.1016/j.rse.2013.03.013, 2013.

Statistic Bulletin on China Water Activities, available at: http://www.mwr.gov.cn/english/publs/202001/t20200102_1384908.html, (last access: 17 December 2021), 2018.

Tavakoly, A. A., Gutenson, J. L., Lewis, J. W., Follum, M. L., Rajib, A., LaHatte, W. C., and Hamilton, C. O.: Direct integration of numerous dams and reservoirs outflow in continental scale hydrologic modeling, Water Resour. Res., 57, e2020WR029544, doi: 10.1029/2020WR029544, 2021.

https://doi.org/10.5194/essd-2021-470
Preprint. Discussion started: 16 May 2022

Tiwari, A.D., and Mishra, V.: Prediction of reservoir storage anomalies in India, J. Geophy. Res. Atmos., 124, 3822–3838, doi: 10.1029/2019JD030525, 2019.

Tortini, R., Noujdina, N., Yeo, S., Ricko, M., Birkett, C. M., Khandelwal, A., Kumar, V., Marlier, M. E., and Lettenmaier, D. P.: Satellite-based remote sensing data set of global surface water storage change from 1992 to 2018, Earth Syst. Sci. Data, 12, 1141-1151, doi: 10.5194/essd-12-1141-2020, 2020.

Villadsen, H., Deng, X., Andersen, O. B., Stenseng, L., Nielsen, K., and Knudsen, P.: Improved inland water levels from SAR altimetry using novel empirical and physical retrackers, J. Hydrol., 537, 234–247, doi: 10.1016/j.jhydrol.2016.03.051, 2016.

Wang, X., Xiao, X., Zou, Z., Dong, J., Qin, Y., Doughty, R. B., Menarguez, M. A., Chen, B., Wang, J., Ye, H, Ma, J., Zhong, Q., Zhao, B., and Li, B.: Gainers and losers of surface and terrestrial water resources in China during 1989–2016, Nat. Commun., 11, 1–12, doi: 10.1038/s41467-020-17103-w, 2020.

Weekley, D., and Li, X.: Tracking multidecadal lake water dynamics with Landsat imagery and topography/bathymetry, Water Resour. Res., 55, 8350–8367, doi: 10.1029/2019WR025500, 2019.

Wingham, D. J., Francis, C. R., Baker, S., Bouzinac, C., Brockley, D., Cullen, R., de Chateau-Thierry, P., Laxon, S. W., Mallow, U., Mavrocordatos, C., Phalippou, L., Ratier, G., Rey, L., Rostan, F., Viau, P., and Wallis, D. W.: CryoSat: A mission to determine the fluctuations in Earth's land and marine ice fields, Adv. Space Res., 37, 841–871, doi: 10.1016/j.asr.2005.07.027, 2006.

Yao, F., Wang, J., Wang, C., and Crétaux, J.-F.: Constructing long-term high-frequency time series of global lake and reservoir areas using Landsat imagery, Remote Sens. Environ., 232, 111210, doi: 10.1016/j.rse.2019.111210, 2019.

Yassin, F., Razavi, S., Elshamy, M., Davison, B., Sapriza-Azuri, G., and Wheater, H.: Representation and improved parameterization of reservoir operation in hydrological and land-surface models, Hydrol. Earth Syst. Sci., 23, 3735–3764, https://doi. org/10.5194/hess-23-3735-2019, 2019.

Yigzaw, W., Li, H. Y., Demissie, Y., Hejazi, M. I., Leung, L. R., Voisin, N., and Payn, R.: A new global storage-area-depth data set for modeling reservoirs in land surface and earth system models, Water Resour. Res., 54, 10–372, doi: 10.1029/2017WR022040, 2018.

Zajac, Z., Revilla-Romero, B., Salamon, P., Burek, P., Hirpa, F. A., and Beck, H.: The impact of lake and reservoir parameterization on global streamflow simulation, J. Hydrol., 548, 552–568, doi: 10.1016/j.jhydrol.2017.03.022, 2017.

Zhang, G., Xie, H., Kang, S., Yi, D., and Ackley, S. F.: Monitoring lake level changes on the Tibetan Plateau using ICESat altimetry data (2003–2009), Remote Sens. Environ., 115, 1733–1742, doi: 10.1016/j.rse.2011.03.005, 2011.

Zhang, S., Gao, H., and Naz, B. S.: Monitoring reservoir storage in South Asia from multisatellite remote sensing, Water Resour. Res., 50, 8927–8943, doi: 10.1002/2014WR015829, 2014.

Zhang, X., Jiang, L., Kittel, C. M. M., Yao, Z., Nielsen, K., Liu, Z., Wang, R., Liu, J., Andersen, O. B., Bauer-Gottwein, P.: On the performance of Sentinel-3 altimetry over new reservoirs: Approaches to determine onboard a priori elevation, Geophys. Res. Letters, 47, e2020GL088770, doi: 10.1029/2020GL088770, 2020.

https://doi.org/10.5194/essd-2021-470
Preprint. Discussion started: 16 May 2022

Zhao, G., and Gao, H.: Automatic Correction of Contaminated Images for Assessment of Reservoir Surface Area Dynamics, Geophys. Res. Letters, 45, 6092–6099, doi: 10.1029/2018GL078343, 2018.

Zhao, G., Gao, H., Naz, B. S., Kao, S. C., and Voisin, N.: Integrating a reservoir regulation scheme into a spatially distributed hydrological model, Adv. Water Resour., 98, 16–31, doi: 10.1016/j.advwatres.2016.10.01, 2016.

Zhong, R., Zhao, T., and Chen, X.: Hydrological model calibration for dammed basins using satellite altimetry information, Water Resour. Res., 56, e2020WR027442, doi: 10.1029/2020WR027442, 2020.

Zhu, J., Song, C., Wang, J., and Ke, L.: China's inland water dynamics: The significance of water body types, Proc. Natl. Acad. Sci. U.S.A., 117, 13876–13878, doi: 10.1073/pnas.2005584117, 2020.